The Sde Phosphoribosyl-Linked Ubiquitin Transferases protect the *Legionella pneumophila* vacuole from degradation by the host.

Running title: Ubiquitin transferases promotes pathogen vacuole integrity

Seongok Kim[a] and Ralph R. Isberg [a,b]

[a]Department of Molecular Biology and Microbiology, Tufts University School of Medicine, 150 Harrison Avenue, Boston, MA 02111, USA

*Corresponding author: Ralph Isberg, Tufts University School of Medicine, 150 Harrison Ave., Boston, MA 02111, United States; email: ralph.isberg@tufts.edu, Phone: 617-636-3993

Author Contributions: S.K.: Performed and designed experiments; performed data analysis; composed manuscript. R.R.I.: Designed experiments; performed data analysis; composed manuscript

Competing Interest Statement: The Authors have no competing interests.

Classification: Biological Sciences > Microbiology

Keywords: *Legionella*; macrophage; intracellular growth; reticulon; vacuoles

Abstract

Legionella pneumophila grows intracellularly within a host membrane-bound vacuole that is formed in response to a bacterial type IV secretion system (T4SS). T4SS translocated Sde proteins promote phosphoribosyl-linked ubiquitination of endoplasmic reticulum protein Rtn4, but the role played by this modification is obscure due to lack of clear growth defects of mutants. To identify the steps in vacuole biogenesis promoted by these proteins, mutations were identified that unmasked growth defects in Δ*sde* strains. Mutations in the *sdhA*, *ridL* and *legA3* genes aggravated the Δ*sde* fitness defect, resulting in disruption of the *Legionella*-containing vacuole (LCV) membrane within 2 hrs of bacterial contact with host cells. Depletion of Rab5B and sorting nexin 1 partially bypassed loss of Sde proteins, consistent with Sde blocking early endosome and retrograde trafficking, similar to roles previously demonstrated for SdhA and RidL proteins. Sde protein protection of LCV lysis was only observed shortly after infection, presumably because Sde proteins are inactivated by the metaeffector SidJ during the course of infection. Deletion of SidJ extended the time that Sde proteins could prevent vacuole disruption, indicating that Sde proteins are negatively regulated at the posttranslational level and are limited to protecting membrane integrity at the earliest stages of replication. Transcriptional analysis was consistent with this timing model for an early point of execution of Sde protein. Therefore, Sde proteins act as temporally-regulated vacuole guards during establishment of the replication niche, possibly by constructing a physical barrier that blocks access of disruptive host compartments early during biogenesis of the LCV.

Significance statement

Maintaining replication compartment integrity is critical for growth of intravacuolar pathogens within host cells. By identifying genetically redundant pathways, *Legionella pneumophila* Sde proteins that promote phosphoribosyl-linked ubiquitination of target eukaryotic proteins are shown to be temporally-regulated vacuole guards, preventing replication vacuole dissolution during early stages of infection. As targeting of reticulon 4 by these proteins leads to tubular endoplasmic reticulum aggregation, Sde proteins are likely to construct a barrier that blocks access of disruptive early endosomal compartments to the replication vacuole. Our study provides a new framework for how vacuole guards function to support biogenesis of the *L. pneumophila* replicative niche.

Introduction

Legionella pneumophila is an intravacuolar pathogen of amoebae that can cause pneumonic disease in susceptible human hosts (1, 2). As a causative agent of Legionnaires' disease, infection is driven by inhalation or aspiration of contaminated water, followed by bacterial growth within alveolar macrophages (3, 4). Failure to clear infection from the lungs in the immunocompromised patient results in life-threatening disease.

Successful intracellular growth in hosts depends on the establishment of the specialized *Legionella*-containing vacuolar (LCV). Upon internalization, more than 300 different effectors are translocated through the Icm/Dot type IV secretion system (T4SS) into host cells (5-9). The Icm/Dot translocated substrates (IDTS) hijack host-membrane trafficking pathways, redirecting components of the host cell secretory system to remodel the pathogen compartment into a replication-permissive LCV (10). Most notable is the ability of the LCV to avoid phagosome maturation as a consequence of association with the endoplasmic reticulum (ER), bypassing fusion with compartments that can lead to either microbial degradation or dissolution of the LCV membrane (10-14). Mutations in the Icm/Dot system prevent LCV formation and block intracellular growth, although deletions of single secreted effectors result in either small or undetectable intracellular replication defects. The inability to uncover intracellular growth defects from loss of single effectors is consistent with genetic redundancy, resulting from multiple substrates targeting a single host membrane trafficking pathway or multiple host pathways working in parallel to support LCV biogenesis (6, 15).

The Sde family (*sdeA*, *sdeB*, *sdeC* and *sidE* in the Philadelphia 1 clinical isolate) is a group of homologous IDTS that contains an N-terminal deubiquitinase (DUB), a nucleotidase/phosphohydrolase (NP) domain, and a central mono-ADP-ribosyltransferase

103 domain (mART). The mART domain ADPribosylates host ubiquitin (Ub) that, in turn, is used as
104 a substrate for the NP domain to promote phosphoribosyl-linked Ub (pR-Ub) modification of
105 target host proteins (16-23). One of the primary targets of the Sde family is host reticulon 4
106 (Rtn4) (19, 22, 24, 25). Phosphoribosyl-Ub modification of Rtn4 promotes endoplasmic
107 reticulum (ER) rearrangements about the LCV within minutes of bacterial contact with host cells
108 (22). Although the absence of Sde family proteins results in small intracellular growth defects in
109 amoebal hosts (26), these defects are subtle during macrophage challenge, consistent with
110 genetic redundancy. This argues that unidentified bacterial translocated effectors may
111 compensate for loss of the Sde family by targeting parallel host pathways that support LCV
112 biogenesis. Redundancy is likely to be limited to the earliest stages of infection, as other IDTS
113 negatively regulate the function of the Sde family. For instance, the mART activity of Sde
114 proteins is inactivated by SidJ, a meta-effector that glutamylates the E860 active site residue (26-
115 29). Furthermore, pR-Ub modification of target proteins is reversed by a pair of pR-Ub-specific
116 deubiquitinases, DupA/B, arguing for temporally limiting Sde family function (24, 25).
117 In this work, we identified proteins that may compensate for loss of Sde function. Chief
118 among them is the T4SS substrate SdhA protein which is required for maintaining membrane
119 integrity of the LCV (30, 31). SdhA binds the OCRL phosphatase involved in the regulation of
120 early and recycling endosomes, and likely diverts these disruptive compartments from interacting
121 with the LCV (32-34). In the absence of SdhA, the bacteria are exposed to host cytosol and
122 subjected to bacterial degradation by interferon-regulated proteins, leading to pyroptotic host cell
123 death (35, 36). RNAi depletion of Rab5, Rab11 and Rab8, which are guanosine triphosphatases
124 (GTPase) involved in regulating the endocytic and recycling endosome pathways, partially

recovers loss of LCV integrity seen in the absence of SdhA, consistent with these compartments disrupting LCV integrity (37).

A second *L. pneumophila* translocated effector that interfaces with the retromer complex is RidL which binds to host VPS29, blocking the function of the retromer which is critical for recycling cargo from endosomes to the trans-Golgi network and to the plasma membrane (38-40). Retrograde trafficking is thought to be blocked by RidL as a consequence of diverting the retromer to sites on the LCV (40), displacing components known to be required for GTP activation of the complex (41).

Using transposon sequencing (Tn-Seq) to unveil redundant effectors involved in LCV biogenesis, we found mutations in three genes (*sdhA*, *ridL* and *legA3*) that aggravate loss of Sde family function. Given the known functions of these effectors, this work argues that Sde proteins act to catalyze formation of a temporally-regulated physical barrier to protect the LCV from attack by host compartments that disrupt the membrane integrity of the replication niche.

Materials and Methods

Bacterial strains, cultures, cells and growth media

L. pneumophila strains were grown in liquid N-(2-acetamido)-2-aminoethanesulfonic acid (ACES) buffered yeast extract (AYE) media or on solid charcoal buffered yeast extract (CYE) media containing 0.4g/l iron (III) nitrate, 0.135 g/ml cysteine, and 1% α-ketoglutaric acid. 40 µg/ml kanamycin, 5% (vol/vol) sucrose, 1 mM IPTG or 5 µg/ml chloramphenicol were added when appropriate. *E. coli* strains were cultured in liquid LB or on solid LB plates supplemented with 50 µg/ml kanamycin or 12.5 µg/ml chloramphenicol when appropriate. Primary bone marrow-derived macrophages (BMDM) from AJ mice were prepared and cultured as described previously (13).

Construction of *L. pneumophila* Transposon mutant library

Electrocompetent (42) *L. pneumophila* Philadelphia-1 strains SK01(*sde*$^{+}$) and SK02 (Δ*sde*) were transformed with 75 ng of pTO100*MmeI* (43) respectively, plated on CYE supplemented with kanamycin and sucrose, and incubated at 37°C for 4 days. Multiple pools were made from each strain, each containing 50,000-80,000 colony forming units (CFUs), which were subsequently harvested and pooled into AYE containing 20% (vol/vol) glycerol. Bacterial suspensions were aliquoted at a concentration ~5 x 10^{9} cfu/ml and stored in -80°C. Each of the pools were subjected to deep sequencing of the insertion sites (Illumina HiSeq 2500) to determine pool complexity, and the resulting information was submitted to NCBI Sequence Read Archive under accession No. PRJNA544499.

Tn-seq screen: Growth of *L. pneumophila* Transposon mutant library in BMDM

Three of the transposon mutant library pools in *L. pneumophila* SK01 (*sde*$^{+}$) and SK02 (Δ*sde*) strains, encompassing 186,340 and 170,822 mutants based on deep sequencing analysis, were independently diluted to A600 = 0.25–0.3, cultured to A600 = 0.3–0.4, diluted back to A600 = 0.2 and cultured in AYE to A600 = 3.8-4.0. Aliquots of each library pool grown in AYE were saved as input samples (T1) for growth in AYE broth, and then used to challenge BMDM at a multiplicity of infection (MOI) = 1 for 24 hrs. Cells were washed 3X at 2 hr post-infection (hpi) with PBS, then replenished with fresh medium and further incubated for 24 hrs. BMDMs were then lysed in H_2O containing 0.05% saponin, and the diluted lysates were incubated on CYE plates with further incubation at 37°C for 3 days. 1-7 X 10^6 colonies were harvested in AYE, mixed thoroughly and used as the output sample (T2) for sequencing analysis. Genomic DNA from input and output samples was extracted using a QIAGEN DNeasy Blood and Tissue kit, including proteinase K prior to insertion-specific amplification and sequencing.

Transposon sequencing and Fitness calculation

Illumina^{TM} sequencing libraries were prepared as described previously (44). Genomic DNA (40 ng) was tagmented in a 10 µl reaction mixtures at 55°C for 5 min, followed by inactivation at 95°C for 30s. 40 µl of PCR mixture (First PCR), including primers 1st_TnR, Nextera2A-R and NEB Q5 high-fidelity polymerase (sequences of primers listed in Supplementary Table 1) was added to the tagmented samples to amplify transposon-adjacent DNA. The PCR amplification was performed by incubating at 98°C for 10 s, 65°C for 20 s and 72°C for 1 min (30 cycles), followed by 72°C for 2 min. After amplification, 0.5 µl of the PCR mixture was used in a second PCR reaction containing nested index primers (LEFT indexing

primer specific for Mariner and RIGHT indexing primer) and Q5 polymerase in 50 µl total volume. The PCR conditions were 98°C for 10s, 65°C for 20s and 72°C for 1 min, followed by 72°C for 2 min. 9 µl of the PCR reaction was loaded and separated on a 1% agarose-Tris-acetate-EDTA (TAE) gel containing SYBR safe dye, and image intensity in the 250-600 bp region was quantified and pooled from each PCR product in equimolar amounts. The multiplexed libraries were purified on Qiagen QIAquick columns, with 17.5 pmol DNA then used in a 50 µl reconditioning reaction with primers P1 and P2 (Supplemental Table 1) and Q5 polymerase. The reaction was subjected to 95°C for 1 min, 0.1°C/s slow ramp to 64°C for 20 s and 72°C for 10 min. After PCR purification, multiplexed libraries were quantified, size-selected (250-600 bp; Pippin HT) and sequenced (single-end 50 bp) by Tufts University Genomics Core Facility. Sequencing was performed using Illumina HiSeq 2500 with high-output V4 chemistry and custom primer with mar512.

Sequencing reads were processed (FASTX-toolkit), mapped to chromosome (AE017354) (Bowtie) and used to calculate individual transposon mutant fitness using a published pipeline (45). The fitness of an individual mutant (W_i) was calculated based on mutant vs population-wide expansion from T1 to T2 with following equation (46).

$$W_i = \frac{\ln(N_i(t_2) \times d / N_i(t_1))}{\ln((1-N_i(t_2)) \times d / (1-N_i(t_1)))},$$

in which $N_i(t_1)$ and $N_i(t_2)$ are the mutant frequency at t_1 and t_2, respectively, and d is the population expansion factor. Transposon insertion sites located in the 5'- and 3'- terminal 10% of the open reading frame and genes having less than 5 insertions were excluded for further analysis.

Construction of *Legionella* deletion mutants

Individual genes were deleted in Lp02 strain by tandem double recombination using the suicide plasmid pSR47s as previously described (47). Primers used to construct all deletion plasmids are listed in Supplementary *SI Appendix* 1, Table S1. Plasmids were propagated in *E. coli* DH5α λpir.

Construction of complementing plasmids

To perform complementation experiments with genes encoded *in trans* on a replicating plasmid, pMMB207Δ267 (15, 48) was digested with *SacI-KpnI* and ligated with PCR-amplified DNA fragments encoding a 6xHis epitope tag, kanamycin resistance gene and *ccdB* flanked by *attR* recombination sites (gift of Tamara O'Connor), which was similarly digested, to generate a Gateway™-compatible destination vector (pSK03; *SI Appendix1*, Table S1). The individual genes were then cloned into the pSK03 plasmid by integrase cloning from a pDONR221-based IDTS plasmid library (49).

Data availability

All sequence data are deposited in the NCBI Sequence Read Archive under accession numbers: PRJNA544499, PRJNA847256 and PRJNA864753 (WGS data).

Code availability

Scripts used for sequencing read analysis can be found at http://github.com/vanOpijnenLab/MaGenTA.

Intracellular growth assays

The intracellular replication of *L. pneumophila* was measured by luciferase activity using *ahpC::lux* derivatives of the WT and Δ*sde* strains(*SI Appendix* 1, Table S1). Bone marrow-derived macrophages (BMDM) were seeded in 96-well tissue culture plates at a density of 1 x 10^5 cells per well in RPMI medium without phenol read, containing 10% FBS (vol/vol) and 2 mM of glutamine. BMDMs were incubated at 37°C containing 5% CO_2 and challenged with *L. pneumophila* Lux^+ strains at a MOI = 0.05, and luminescence was monitored every 30 min for 3 days during continuous incubation in an environmentally-controlled luminometer (Tecan).

Quantitative RT-PCR

PMA-differentiated U937 cells were seeded at a density of 4 x 10^6 cells per well in 6 well tissue culture plates. Cells were infected with post-exponentially grown *L. pneumophila* Lp02 at a MOI = 20 and washed at 1 hpi. RNA was isolated using Trizol in accordance with manufacturer's instructions. Contaminating genomic DNA was removed using the TURBO DNA-free kit, and cDNA was synthesized with 2.5 µg of RNA using SuperScript VILO cDNA Synthesis Kit. PowerUp SYBR Green Master Mix was then used for qRT-PCR reactions using Second Step instrument (ABI). Transcriptional levels of genes were normalized to 16S rRNA. Oligonucleotides are listed in *SI Appendix* 1, Table S1.

Cytotoxicity assays

10^5 BMDMs were seeded per well in 96 well tissue culture plates and incubated overnight at 37°C, 5% CO_2 prior to replenishing with 100 µl of medium containing propidium iodide (PI) at a final concentration = 20 µg/ ml. Cells were challenged with 100 µl of

256 postexponentially grown *L. pneumophila* Lp02 in the same medium at a MOI = 1 or 5 (36).
257 Following infections, cells were centrifuged at 400 x g for 5 mins, incubated at 37^{o}C, 5% CO_2,
258 and PI uptake was monitored every 10 min using the bottom reading setting in an
259 environmentally controlled fluorometer (Tecan). To determine 100% cytotoxicity as the
260 normalization control, cells were treated with 0.1% Triton X-100, and PI uptake was determined.
261
262 **Assay for vacuole integrity**
263 To measure the fraction of infected cells having intact *Legionella*-containing vacuoles
264 (LCV), bacteria were centrifuged onto BMDMs for 5 min and incubated at 37^{o}C, 5% CO_2 for
265 noted periods of time. The infection mixtures were then fixed in PBS containing 4%
266 paraformaldehyde, then probed with mouse anti-*L. pneumophila* (Bio-Rad, Cat# 5625-0066,
267 1:10,000) followed by secondary probing with goat anti- mouse Alexa Fluor 594 (Invitrogen,
268 Cat# A11005, 1:500), to identify permeable vacuoles as described (31). After washing 3X in
269 PBS, LCVs were permeabilized by 5 min incubation with -20^{o}C methanol, prior to a second
270 probing with mouse anti-*L. pneumophila*. All bacteria (both from intact and disrupted vacuoles)
271 were identified by goat anti-mouse IgG Alexa Fluor 488 (Invitrogen, Cat# A11001, 1:500). The
272 amount of vacuole disruption was quantified in two fashions. First, individual BMDMs were
273 imaged using Zeiss observer Z1at 63X and scored for permeabilization based on staining with
274 goat anti-mouse IgG-AlexaFluor 594 (antibody accessible in absence of methanol
275 permeabilization) as described previously (32) . To allow larger numbers of infected cells to be
276 imaged, automated microscopy was performed using the Lionheart FX scanning microscope and
277 Gen5 image prime 3.10 software. For detection of disrupted vacuoles (permeable in absence of
278 methanol treatment), all images were analyzed by image preprocessing (10X magnification). To

279 determine colocalization and quantification of vacuole integrity at 2 hpi, a primary mask was set
280 for goat anti-mouse IgG-AlexaFluor 488 (detected after methanol treatment) and a secondary
281 mask was set using a region that was expanded approximately 0.001 µm from the primary mask
282 for goat anti-mouse IgG Alexa Fluor 594 (detected before methanol treatment). To identify
283 intracellular bacteria, DAPI staining of nuclei was used to threshold a secondary mask 4 µm
284 apart from the primary mask.
285
286 **RTN4 colocalization with LCV**
287 RTN4 colocalization with the LCV was assayed by immunofluorescence microscopy.
288 BMDMs were infected with *Legionella* strains for 4 hrs, fixed in PBS containing 4%
289 paraformaldehyde, then extracted in 5% SDS to remove most of the cell-associated RTN4, then
290 probed with mouse anti-*L. pneumophila* (Bio-Rad, Cat# 5625-0066, 1:10,000) and rabbit anti-
291 RTN4 (Lifespan Biosciences, Cat# LS-B6516, 1:500) to detect detergent-resistant structures
292 about the LCV. Bacteria were detected with anti-mouse Alexa fluor-594 and RTN4 structures
293 with anti-rabbit Alexa Fluor-488 (Jackson ImmunoResearch, Cat# 711-545-152, 1:250).
294
295 **Nucleofection**
296 Differentiated BMDMs were seeded at a density of 5 x 10^6 cells in 10 cm dishes filled
297 with 10 mls RPMI medium containing 10% FBS and 10% supernatant produced by 3T3-
298 macrophage colony stimulating factor (mCSF) cells (50) and incubated overnight. Cells were
299 lifted in cold PBS and resuspended in RPMI medium containing 10% FBS. Resuspended cells
300 were aliquoted into 1.5 ml microfuge tubes containing 1 x 10^6 cells and pelleted at 200 x g for 10
301 min. The pellets were resuspended in nucleofector buffer (Amaxa Mouse Macrophage

Nucleofector Kit, Cat# VPA-1009) and 2 μg of siRNA was added (siGENOME smart pool, Dharmacon). Cells were transferred to a cuvette and nucleofected in the Nucleofector 2b Device using Y-001 program settings according to manufacturer's instructions. Nucleofected macrophages were immediately recovered in the medium and plated in 8-well chamber slides at 5 x 10^4 /well for microscopy assays or in 12-well plates at 1.5 x 10^5/well to prepare cell extracts for immunoblotting.

Immunoblotting

The efficiency of siRNA silencing in nucleofected cells was determined by immunoblot probing of SDS-PAGE fractionated proteins. Necleofected macrophages plated in 12-well plates were lysed by incubating in RIPA buffer (Thermo Fisher Scientific, Cat#89900) for 20 min on ice and protein concentration was measured by BCA assay. 5-10 μg of protein in SDS-PAGE sample buffer was boiled for 10 min, fractionated by SDS-PAGE and transferred to nitrocellulose membranes. The membrane was blocked in 50 mM Tris-buffered saline/0.05% Tween 20 (TBST, pH 8.0) containing 4% nonfat milk (blocking buffer) for 1 hr at room temperature and probed with primary antibodies against Rab5B (Proteintech, Cat# 27403-1-AP, 1:1,000), SNX1 (Proteintech, Cat# 10304-1-AP, 1:1000), RTN4 (Lifespan Biosciences, Cat# LS-B6516, 1:2,000), polyHistidine (Sigma-Aldrich, Cat# H1029, 1:2,000) and β-actin (Invitrogen, Cat# PA1-183, 1:1,000) in blocking buffer at 4°C overnight. After washing 3X with TBST, the membranes were incubated with secondary antibody (Li-Cor Biosciences, Cat#926-32211, 1: 20,000) in blocking buffer for 45 min at room temperature. Capture and analysis were performed using Odyssey Scanner and the image Studio software (LI-COR Biosciences).

Results

Identification of genes involved in LCV biogenesis that can compensate for the loss of Sde

We previously demonstrated that the *L. pneumophila* Δ*sde* strain (Δ*sidE* Δ*sdeABC*) is partially defective for growth within protozoan hosts, but grows in murine macrophages at levels close to that of the *L. pneumophila* WT strain (22, 51). This phenomenon is consistent with the existence of redundant Icm/Dot translocated substrates (IDTS) that can compensate for the lack of Sde proteins in mammalian hosts (15). To identify redundant pathways involved in intracellular growth, we performed transposon sequencing (Tn-seq) mutagenesis to uncover mutations that aggravate the Δ*sde* intracellular growth defect within bone marrow-derived macrophages (BMDMs). Transposon library pools were generated in both the WT and the Δ*sde* strain using the *Himar1* transposon which specifically inserts at TA dinucleotides (52).

Three independently collected pools of *Himar-1* insertions were constructed in the *L. pneumophila* WT and Δ*sde* strains, encompassing 117,419 (47.33% of total TA sites) and 108,934 (43.91% of total TA sites) total unique insertions in the two genomes, respectively. This represented approximately 34 and 31 insertions/gene in WT and Δ*sde*, respectively (Dataset S1). After growth in broth to post-exponential phase (T1) (53), BMDMs were challenged with both pools for 24 hr (equivalent to a single round of infection; T2) and the fitness contribution of each mutation was determined during growth in broth and in BMDMs (Fig. 1A; Materials and Methods) (46). To identify genes that were required for intracellular replication in macrophages, the fitness difference between BMDM growth versus nutrient-rich medium growth was calculated in the WT and Δ*sde* strains, respectively (Figs. 1B, C). Insertions in the majority of genes that were nonessential for growth in broth exhibited a fitness of ~1 during 24 hr incubation in BMDMs, indicating that most genes are not required for intracellular growth in macrophages

(*SI Appendix* 1, Fig. S1). It has been established that individual loss of only 6 IDTS (*mavN*, *sdhA*, *ravY*, Lpg2505, *legA3* and *lidA*) impair growth in macrophages, while individual loss of most of the other 300+ effectors show little defect in intracellular growth. This has been attributed to functional redundancy in *Legionella* secreted effectors (10, 30, 54-57). In our datasets, we confirmed those genes were required for replication in macrophages in WT (Fig. 1B, indicated by blue lettering). Furthermore, mutations in the preponderance of genes encoding translocator effectors generated no statistically significant defects in intracellular growth in either of the two backgrounds (Figs. 1B, C), consistent with previous studies.

We then filtered mutations based on the following criteria: 1) causing lowered fitness relative to the population median, as defined by modified Z score > 1 (median absolute deviation (MAD) >1) and $p < 0.05$ based on unpaired t tests comparing mutations in the WT vs. Δ*sde* background (Dataset S1); 2) genes encoding *Icm/Dot* translocated substrates; and 3) genes encoding proteins thought to be involved in LCV biogenesis, based on published data. In addition, we identified mutations that showed no statistical defect in the WT, but whose fitness difference (Δ*sde* - WT) was > 1 MAD from the population median without any other consideration. Based on these criteria, 3 genes (*sdhA*, *ridL* and *legA3*) were prioritized for further analysis (Fig. 1D). SdhA protein is a T4SS substrate required for maintaining LCV integrity (30, 31). The absence of *sdhA* caused a growth defect in BMDMs infected with either WT or the Δ*sde* strains (Fig. 1B, C). Even so, the fitness defect was significantly aggravated when *sdhA* was disrupted in the Δ*sde* strains relative to its loss in a WT strain background (Fig. 1D).

Mutations in *ridL* or *legA3* also showed aggravating growth defects in the Δ*sde* strains (Fig. 1D). RidL is a T4SS substrate that can inhibit function of the retromer complex that modulates retrograde traffic from early endosomes (40, 58). LegA3 is an ankyrin-repeat effector

371 protein that is required for optimal replication in several hosts that has not been clearly tied to
372 replication vacuole formation previously (15, 38, 43). Defective growth was specific to BMDMs
373 as the double mutant strains grew as well as the WT strain in bacteriological medium (Fig. 1E
374 and Dataset S1). Most notably, based on their efficient growth in a WT background, was the
375 behavior of insertions in *ridL*, which showed clear defects in a Δ*sde* background (Figs. 1C, D)

376 **The absence of Sde proteins exacerbates intracellular growth defects of *sdhA*, *ridL* or *legA3***
377 **deletion mutants.**

378 To verify that the phenotypes predicted by the parallel Tn-seq pools can be reproduced at
379 the single strain level, in-frame deletion mutations in *sdhA, ridL and legA3* were generated in
380 both the WT and Δ*sde* strain backgrounds harboring the luciferase (*ahpC*::*lux*$^{+}$) reporter. The
381 respective mutations were confirmed by whole genome sequencing (PRJNA864753), and
382 intracellular growth of *L. pneumophila* strains was then monitored by luminescence
383 accumulation after incubation with BMDMs. As predicted by the Tn-seq analysis, combining the
384 loss of Sde proteins with the Δ*ridL* mutation revealed a growth defect that did not exist in the
385 absence of the combination. In the presence of the Sde proteins, the Δ*ridL* strain showed no
386 growth defect after challenge of BMDMs. In contrast, introduction of Δ*ridL* into the Δ*sde* strain
387 resulted in yields that were 100X lower relative to the WT and approximately 10X lower relative
388 to the parental Δ*sde* strain after 72 hr incubation (Fig. 2A). Additionally, catastrophic synergistic
389 defects were observed with the Δ*legA3* mutation after introduction into the Δ*sde* background. In
390 an otherwise WT background, loss of either Sde proteins or RidL resulted in mild growth defects
391 after 72 hours incubation. The Δ*sde*Δ*legA3* strain, however, showed little or no evidence of
392 growth during this time period (Fig. 2B). Finally, although the Δ*sdhA* strain reproduced the

393 previously documented growth defect in BMDMs (30, 31), combination with Δ*sde* resulted in a
394 strain that showed yields similar to the type IV secretion system defective *dotA*$^-$ strain (Fig. 2C)
395
396 **Aggravation of the Δ*sde* lesion causes premature host cell death due to destabilization of**
397 **the LCV.**
398 To determine if there were a clear defect in replication vacuole biogenesis associated
399 with aggravating the loss of Sde function, we took advantage of the fact that SdhA is required to
400 maintain integrity of the LCV, reasoning that the absence of Sde could exacerbate this defect (31,
401 32). As had been noted previously, challenge with a Δ*sdhA* strain resulted in a significant
402 fraction of the LCVs becoming permeable and accessible to antibody penetration at 6 hours post-
403 infection (hpi) (*SI Appendix* 1, Fig. S2) (31). At 2 hpi, however, there is no evidence that the
404 absence of SdhA interferes with LCV integrity, with both the WT and Δ*sdhA* strains showing
405 indistinguishable levels of permeability to antibody staining (*SI Appendix* 1, Fig. S2). As Sde
406 proteins act to remodel Rtn4 about the replication vacuole within 10 min of bacterial challenge
407 (31, 51), we reasoned that any compensation for loss of SdhA should occur at early timepoints.
408 Therefore, we sought to examine the integrity of the LCV in BMDMs at 2 hpi.
409 Vacuole integrity of the mutants was evaluated by probing fixed BMDM with anti-*L.*
410 *pneumophila* in the presence or absence of chemical permeabilization, using our previously
411 established immunofluorescence staining method (Fig. 3A) (31). Surprisingly, even the Δ*sde*
412 single mutant strain generated a higher frequency of permeable vacuoles than WT at the 2 hr
413 timepoint (Fig. 3B). In contrast, *ridL*, *legA3* and even *sdhA* single deletions showed vacuole
414 permeability frequencies that were comparable to WT at this timepoint (Fig. 3B). The most
415 dramatic effects were observed when deletions of *sdhA*, *ridL*, and *legA3* were introduced into the

Δ*sde* strain. Addition of each individual deletion to the Δ*sde* mutant severely aggravated the vacuole integrity defect, resulting in up to 4-fold more permeable vacuoles, indicating that these mutation combinations drastically destabilized the LCV (Fig. 3B). To allow larger numbers of LCVs to be analyzed (1000 to 3000 per biological replicate), albeit at lower resolution, we used a lower power objective to repeat the analysis. Although low power analysis made it more difficult to identify permeable vacuoles, the results were in concordance with those displayed in Fig. 3B (*SI Appendix* 1, Fig. S3). These results indicate that at early timepoints after infection, the *L. pneumophila* has redundant T4SS substrates that can compensate for the loss of Sde, and that vacuole disruption resulting from absence of *sde* is potentiated by the addition of secondary mutations in *sdhA*, *ridL* and *legA3*.

Pyroptotic cell death occurs as a consequence of a comprised LCV membrane followed by bacterial exposure to the macrophage cytosol (31). Based on the loss of LCV barrier function shortly after initiation of infection, we hypothesized that the respective Δ*sdhA*Δ*sde*, Δ*legA3*Δ*sde* and Δ*ridL*Δ*sde* double mutant strains should accelerate BMDM cell death in comparison to either the WT or single mutants. To this end, cytotoxicity assays were performed, assaying for propidium iodide (PI) access to the macrophage nucleus (Materials and Methods; (36)). In perfect concordance with the loss of LCV integrity, pyroptotic cell death was exacerbated when mutations in either *sdhA*, *ridL* and *legA3* were combined with Δ*sde* (Fig. 3C). Accessibility to PI was more rapid than that observed with the WT and the total cytotoxicity plateaued at levels that far exceeded the WT during the course of the experiment, consistent with the early defect of these double mutants resulting in increased overall damage to the LCV relative to the WT.

Downmodulation of Sde activity by SidJ interferes with vacuole protection

To demonstrate that expression of single Sde effectors was sufficient to restore LCV integrity in the absence of SdhA function, plasmids encoding individual effectors were introduced into the Δ*sde*Δ*sdhA* strain. As expected, the introduction of plasmid-encoded *sdhA* resulted in increased LCV stability, as measured by the antibody accessibility assay (Fig. 4A). Plasmids encoding single Sde effectors (*sdeA*, *sdeB*, *sdeC*: Fig. 4A) allowed similar levels of LCV protection to that observed for the *sdhA*-harboring plasmid. We conclude that each of the Sde proteins demonstrated previously to catalyze phosphoribosyl-linked ubiquitination of Rtn4 and promote associated Rtn4 rearrangements (Fig. 4B; (22)) is sufficient to allow protection of the LCV from degradation.

Sde proteins are only able to compensate for loss of SdhA at early times after infection of BMDMs as there was an accumulation of degraded LCVs in the Δ*sdhA* strain even in presence of Sde at later time points (*SI* Appendix 1, Fig. S2; (31)). An explanation for this phenomenon is that protection of the LCV by Sde proteins is negatively regulated in a temporal fashion by the SidJ meta-effector which shuts down Sde activity by glutamylation of the mART domain (E860 residue on SdeA; (28)). The primary consequence of this post-translational modification is that Sde proteins are released from the LCV (26), but active SidJ shutdown of phosphoribosyl-linked ubiquitination is also predicted to prevent accumulation of proteins such as Rtn4 about the LCVs. Therefore, the absence of SidJ should both prolong Sde activity and act to compensate for loss of SdhA as the infection proceeds beyond the 4 hr timepoint. To test this hypothesis, a deletion of *sidJ* was introduced into the Δ*sdhA* strain and vacuole integrity was examined at 4 hpi (Fig. 4C). Based on the antibody protection assay, at 4 hpi there was ~33% reduction in degraded vacuoles as a consequence of removing SidJ from the Δ*sdhA* strain (Fig. 4C; compare Δ*sidJ*Δ*sdhA* to Δ*sdhA*).

462 Deletion of SidJ did not completely protect from vacuole disruption, as there were clearly
463 more intact vacuoles after infection with $SdhA^{+}$ strains, indicating that pR-Ub-linked targets
464 likely persist for extended periods of time in the presence of intact SidJ function (WT compared
465 to Δ*sidJ*Δ*sdhA*; Fig. 4C). One likely candidate for persistent modification is RTN4 (Fig. 4D),
466 which forms detergent-resistant aggregates that may slowly dissipate in the absence of continued
467 modification by Sde proteins. To determine if restoration of vacuole disruption is connected to
468 partial loss of RTN4 aggregates, the intensity of Rtn4 aggregates around the LCV was quantified
469 microscopically after detergent extraction (Materials and Methods). Consistent with expectations,
470 the total RTN4 intensity (area plus unit intensity) was increased by removing SidJ (Fig. 4E). The
471 effect was independent of the presence of the *sdhA*, as in both WT (Fig. 4E; WT vs Δ*sidJ*) and
472 Δ*sdhA* strains (Fig. 4E; Δ*sdhA* vs. Δ*sidJ*Δ*sdhA*) the absence of SidJ results in higher levels of
473 Rtn4 accumulation at 4 hpi. Therefore, loss of SidJ lengthens the time that Sde function can
474 compensate for loss of SdhA and is associated with increased accumulation of Rtn4 at this
475 timepoint.
476
477 **LCVs harboring strains lacking *sde* are stabilized by depletion of proteins involved in early**
478 **endocytic and retrograde trafficking.**
479 Based on work from both *Salmonella* and *Legionella*, the most common explanation for
480 bacterial mutants that result in destabilization of the pathogen replication vacuole is that there is
481 a failure to protect from association with host membrane compartments that result in vacuole
482 degradation (37, 59). For example, SdhA antagonizes function of the early endocytic
483 compartment, in part by diverting the OCRL phosphatase (32, 37). As a consequence, depletion
484 of components that regulate early endocytic dynamics, such as Rab5bB, prevents LCV

485 degradation, stabilizing the replication niche in the absence of SdhA (32, 37, 60, 61). To
486 determine if Sde and SdhA proteins protect the LCV from attack by the same host membrane
487 trafficking pathways, depletion with small interfering RNA (siRNA) against Rab5B in BMDMs
488 was performed and vacuole integrity was measured at 2 hpi. At this timepoint, when Sde proteins
489 appear to be the primary stabilizers of the LCV, knockdown of Rab5B partially reversed vacuole
490 disruption after challenge with the Δ*sdhA*Δ*sde* strain (Fig. 5A). This indicates that Sde and SdhA
491 are likely able to interfere with the same early endocytic pathway. As expected, no restoration
492 was observed in cells infected with WT, although the corresponding single Δ*sde* strain, which
493 shows a small defect in maintaining vacuole integrity, was unaffected by the loss of Rab5B (Fig.
494 5A). Therefore, in the absence of Rab5B, there may be another pathway that Sde proteins
495 directly antagonize to promote vacuole integrity.

496 We previously demonstrated that knockdown of Rab11, a GTPase that regulates the
497 recycling endosome, partially rescues the vacuole integrity defect of a Δ*sdhA* strain. This
498 indicates that host recycling compartments interfere with vacuole integrity (37). Furthermore,
499 Sorting Nexin 1 (SNX1) participates in these events, and functions in tandem with the Retromer,
500 which is a target of RidL (39, 40, 62). We thus predicted that the depletion of SNX1 should also
501 reverse vacuole disruption. To this end, SNX1 was depleted by siRNA prior to bacterial infection
502 and vacuole integrity was measured at 2 hpi. In this case, the ability to partially rescue the
503 vacuole integrity defect at an early timepoint was independent of *sdhA* function. For both the
504 Δ*sde* and Δ*sde*Δ*sdhA* strain backgrounds, depletion of SNX1 resulted in a significant reduction
505 of disrupted vacuoles, with 50% and 38% fewer antibody-permeable vacuoles observed in the
506 presence of siRNA directed toward SNX, respectively, when compared to treatment with the
507 scrambled control (Fig. 5B). These results support previous work that early endosome dynamics

508 are involved in disrupting the LCV and are consistent with Sde proteins playing a special role in
509 blocking SNX1/retromer-mediated membrane traffic at early timepoints after bacterial challenge
510 of primary macrophages.
511
512 **Temporally regulated IDTS maintain LCV integrity during infection.**
513 Sde proteins act immediately after contact of bacteria with mammalian cells to promote
514 Rtn4 rearrangements and maintain LCV integrity (22). In contrast, SdhA acts when Sde activity
515 appears to dissipate due to continued action of SidJ (Fig. 4; (26-29), as a Δ*sdhA* strain requires
516 four hours to exhibit a clear defect in LCV integrity. Therefore, these proteins likely execute
517 their roles sequentially, with Sde proteins functioning as vacuole guards at the earliest stages of
518 replication compartment formation, while SdhA works downstream at later time points. To
519 support this sequential function, we hypothesized that there should be temporal regulation of the
520 vacuole guards identified here. To this end, we measured the relative transcription of the vacuole
521 guards after bacterial contact of a WT strain with cultured cells. The expression of *sdeA* and
522 *sdeC* was high at 1 hpi and then dramatically decreased by about 10-fold at 6 hpi compared to
523 that at 1 hpi (Fig. 6). Expression of SidJ was maintained, or raised gradually throughout the
524 infection, consistent with its role in downmodulating Sde function. As found previously, the
525 level of *ridL* expression gradually receded from 1 to 6 hpi (Fig. 6; (40)). In contrast, the
526 expression of *sdhA* and *legA3* increased during infection, by 4- or 10-fold respectively, at 6 hpi
527 (Fig. 6A). These results are consistent with SdhA and LegA3 playing critical roles in preserving
528 LCV integrity at infection times that extend beyond the initial establishment of the LCV (~4 hr)
529 (31).

Discussion

Replication vacuole integrity is a critical determinant of successful pathogen growth within membrane-bound compartments (63). The importance of this process has been demonstrated for several intracellular pathogens, all of which encode proteins critical for maintaining an intact vacuolar barrier (31, 64-66). In each case, bacterial proteins appear to interfere with the function of membranes exiting from early endosomal/recycling compartments (32, 37, 40). There is no clear explanation for how endosomal membranes disrupt replication compartments, but bacterial mutant studies indicate that the replication vacuole has a unique membrane composition that is destabilized by endosomal membranes (67). In particular, *S. typhimurium* and *L. pneumophila* mutants lacking specific phospholipases stabilize these compartments (31, 68). In the case of *L. pneumophila plaA* mutations, loss of a lysophospholipase reduces the fraction of permeable LCVs observed in *sdhA* mutants, indicating that modulation of lysophospholipid content may maintain replication vacuole integrity. In fact, analysis of the *L. pneumophila* translocated effector VpdC argues that lysophospholipid content regulates LCV expansion, consistent with vacuole integrity being dependent on homeostatic control of lysophospholipids (69).

In this report, we obtained the surprising result that the *L. pneumophila* Sde proteins contribute to maintaining LCV integrity (Fig. 2), consistent with their blocking endosomal membrane traffic (Fig. 5). Loss of SdhA or RidL aggravated the minor growth defect of a Δ*sde* strain, thereby eliminating proteins that interface directly with endosomal factors (Fig. 1). In the case of SdhA, the protein engages and diverts the OCRL phosphatase endosomal traffic regulator, while RidL prevents activation of retromer components that modulate retrograde traffic from endosomes (32, 40, 41, 58). Sde proteins may work in a very different fashion than these two

553 proteins. Sde proteins catalyze phosphoribosyl-linked modification of a large number of host
554 proteins, modifying Ser and perhaps Tyr residues on protein targets (19, 70). An early target is
555 the endoplasmic reticulum protein Rtn4, which is not known to directly interface with the
556 endosomal system (22). Largescale identifications of proteins modified by SdeA confirm that
557 Rtn4 is among the most abundant pR-UB-linked proteins (24, 25).

558 The connection between ER rearrangements and support of membrane integrity raises the
559 possibility that Sde action protects the LCV from host attack by forming a shield about the LCV.
560 Immediately after *L. pneumophila* contact with mammalian cells, Sde proteins drive abundant
561 accumulation of Rtn4-rich tubular ER aggregates (Fig. 7). These structures result in complex
562 pseudovesicular structures, observed over 20 years ago in both mammalian cells and amoebae
563 within 10 minutes post-infection (14, 22, 71). Over time, these structures dissipate and are
564 replaced by rough ER (14, 71). Therefore, regulation of Sde function ensures that it operates
565 primarily during the initial stages of replication. This explains why loss of SdhA has little effect
566 on LCV integrity during the first 2 hpi (Fig. 3), and only shows a defect when combined with
567 loss of Sde function. Therefore, SdhA primarily plays a backup role in the first 2 hpi (Fig. 7), but
568 when Rtn4-rich pseudovesicular structures dissipate at later time points (22, 51), SdhA assumes
569 its role as the primary essential guard against LCV disruption.

570 Based on these results, we propose a model in which Sde, RidL and SdhA promote LCV
571 integrity in a temporally controlled fashion (Fig. 7). Shortly after infection, we hypothesize that
572 the Sde proteins act to wall off the LCV from endosomal attack by rearranging tubular ER into
573 dense structures as a consequence of pR-UB-modification of Rtn4 (22). RidL and SdhA are
574 present on the LCV to protect against occasional breaches of this barrier at early time points (32,
575 40). The continued presence of the physical barrier, however, is likely to pose problems for

supporting bacterial growth because it prevents access of the LCV to either metabolites or lipid biosynthesis components. This predicts that optimal growth of *L. pneumophila* must involve the breakdown of the pR-Ub-modified physical barrier. Therefore, metaeffectors that reverse Sde family function, such as the SidJ protein (27-29), are necessary for optimal intracellular growth because they facilitate barrier breakdown (26, 72). Consistent with this model, there is suboptimal growth in the absence of SidJ (26, 72), with the negative consequence that *L. pneumophila sidJ*$^-$ mutants accumulate Rtn4 at the 6 hr timepoint (Fig. 5). To avoid a tradeoff between supporting vacuole integrity and interfering with intracellular growth, *L. pneumophila* has acquired the ability to disrupt the Sde-promoted barrier, necessitating the localization of the SdhA vacuole guard on the LCV to protect a newly established point of vulnerability for the replication niche (Fig. 7).

This work provides a fresh view of the role of redundancy in an intracellular pathogen. In the case of protecting LCV integrity, our work argues that multiple proteins do not work in parallel pathways toward the same end. Instead, each pathway is temporally controlled, playing an important role at different times in the replication process. This then explains the profound replication defect of a *sdhA*$^-$ strain, which only has some low-level support from RidL and residual remnants of the Sde-targeted protein blockade. The lack of effective backup pathways as the replication cycle proceeds necessitates the up-regulation of SdhA, resulting in a largely nonredundant role for this protein (Fig. 6). That RidL and LegA3 are not particularly effective backups for SdhA as the infection cycle proceeds, indicates that these proteins may be unable to block critical membrane-disruptive pathways that are inactivated by SdhA.

An important caveat to this model is that Sde protein can target a number of proteins other than Rtn4 (16, 24, 25). Furthermore, Sde localization is not restricted to the LCV, but

family members can be found on a number of organelles, including endosomes/lysosomes and mitochondria at early stages of infection (~ 1 hr post-infection) (26). In this regard, we think it likely that there are two modes of action that can promote vacuole integrity. One mode is to establish a physical barrier around the LCV by eliciting Rtn4-ER rearrangements. The other is to modify host proteins associated with endocytic trafficking, Golgi biogenesis or autophagy (25). In this regard, partial rescue of the LCV integrity defect by depletion of SNX1 in BMDMs infected with Δ*sde* mutants is particularly noteworthy (Fig. 5C). Previous studies have shown that SNX1 is localized on LCVs, raising the possibility that proteins controlling the movement, docking and fusion of disruptive compartments could come in contact with Sde proteins and allow inactivation of these compartments (25, 40). Therefore, Sde proteins may act as their own backup factors, inactivating disruptive compartments that sneak through the Rtn4-aggregated barrier.

In summary, by performing parallel dense transposon mutagenesis in matched strains, we have obtained evidence that the Sde family acts to protect the LCV from disruption by the host. Furthermore, our study provides a new framework for vacuole guard function, as the described guards are temporally regulated to maximize the replication potential of *L. pneumophila*. Future work will focus on how manipulation of host membrane compartments leads to maintaining LCV integrity, and determining the molecular details for how LCV disruption occurs in the absence of vacuole guards.

Acknowledgements. We thank Dr. Joseph Vogel for the kind gift of the *Legionella* strain (Δ*sidJ*), Drs. Ila Anand and Mengyun Zhang for preliminary work indicating that SNX1 contributes to driving LCV disruption, and Dr. Philipp Aurass for discussions regarding analysis of Tn-seq results. We thank Juan Hernandez-Bird, Mitchell Berg, and Drs. Wenwen Huo, Philipp

622 Aurass and Kevin Manera for review of the text. This work was supported by NIAID Awards

623 5R01-AI46245 and 5R01-AI113211 to RRI.

624

625

626

References

1. T. J. Rowbotham, Preliminary report on the pathogenicity of *Legionella pneumophila* for freshwater and soil amoebae. *J Clin Pathol* **33**, 1179-1183 (1980).
2. T. W. Nash, D. M. Libby, M. A. Horwitz, Interaction between the Legionnaires' disease bacterium (*Legionella pneumophila*) and human alveolar macrophages. Influence of antibody, lymphokines, and hydrocortisone. *J Clin Invest* **74**, 771-782 (1984).
3. T. M. Nguyen *et al.*, A community-wide outbreak of Legionnaires disease linked to industrial cooling towers--how far can contaminated aerosols spread? *J Infect Dis* **193**, 102-111 (2006).
4. M. A. Horwitz, S. C. Silverstein, Legionnaires' disease bacterium (*Legionella pneumophila*) multiples intracellularly in human monocytes. *J Clin Invest* **66**, 441-450 (1980).
5. W. Zhu *et al.*, Comprehensive identification of protein substrates of the Dot/Icm type IV transporter of *Legionella pneumophila*. *PLoS One* **6**, e17638 (2011).
6. Z. Q. Luo, R. R. Isberg, Multiple substrates of the *Legionella pneumophila* Dot/Icm system identified by interbacterial protein transfer. *Proc Natl Acad Sci U S A* **101**, 841-846 (2004).
7. L. Huang *et al.*, The E Block motif is associated with *Legionella pneumophila* translocated substrates. *Cell Microbiol* **13**, 227-245 (2011).
8. Z. Lifshitz *et al.*, Computational modeling and experimental validation of the *Legionella* and *Coxiella* virulence-related type-IVB secretion signal. *Proc Natl Acad Sci U S A* **110**, E707-715 (2013).
9. L. Gomez-Valero *et al.*, More than 18,000 effectors in the *Legionella* genus genome provide multiple, independent combinations for replication in human cells. *Proc Natl Acad Sci U S A* **116**, 2265-2273 (2019).
10. R. R. Isberg, T. J. O'Connor, M. Heidtman, The *Legionella pneumophila* replication vacuole: making a cosy niche inside host cells. *Nat Rev Microbiol* **7**, 13-24 (2009).
11. E. Haenssler, V. Ramabhadran, C. S. Murphy, M. I. Heidtman, R. R. Isberg, Endoplasmic Reticulum Tubule Protein Reticulon 4 Associates with the *Legionella pneumophila* Vacuole and with Translocated Substrate Ceg9. *Infect Immun* **83**, 3479-3489 (2015).
12. J. C. Kagan, C. R. Roy, *Legionella* phagosomes intercept vesicular traffic from endoplasmic reticulum exit sites. *Nat Cell Biol* **4**, 945-954 (2002).
13. M. S. Swanson, R. R. Isberg, Association of *Legionella pneumophila* with the macrophage endoplasmic reticulum. *Infect Immun* **63**, 3609-3620 (1995).
14. L. G. Tilney, O. S. Harb, P. S. Connelly, C. G. Robinson, C. R. Roy, How the parasitic bacterium *Legionella pneumophila* modifies its phagosome and transforms it into rough ER: implications for conversion of plasma membrane to the ER membrane. *J Cell Sci* **114**, 4637-4650 (2001).
15. T. J. O'Connor, D. Boyd, M. S. Dorer, R. R. Isberg, Aggravating genetic interactions allow a solution to redundancy in a bacterial pathogen. *Science* **338**, 1440-1444 (2012).
16. Y. Liu *et al.*, Serine-ubiquitination regulates Golgi morphology and the secretory pathway upon *Legionella* infection. *Cell Death Differ* **28**, 2957-2969 (2021).
17. A. Akturk *et al.*, Mechanism of phosphoribosyl-ubiquitination mediated by a single *Legionella* effector. *Nature* **557**, 729-733 (2018).

18. Y. Dong *et al.*, Structural basis of ubiquitin modification by the *Legionella* effector SdeA. *Nature* **557**, 674-678 (2018).
19. S. Kalayil *et al.*, Insights into catalysis and function of phosphoribosyl-linked serine ubiquitination. *Nature* **557**, 734-738 (2018).
20. Y. Wang *et al.*, Structural Insights into Non-canonical Ubiquitination Catalyzed by SidE. *Cell* **173**, 1231-1243 e1216 (2018).
21. J. Qiu *et al.*, Ubiquitination independent of E1 and E2 enzymes by bacterial effectors. *Nature* **533**, 120-124 (2016).
22. K. M. Kotewicz *et al.*, A Single *Legionella* Effector Catalyzes a Multistep Ubiquitination Pathway to Rearrange Tubular Endoplasmic Reticulum for Replication. *Cell Host Microbe* **21**, 169-181 (2017).
23. S. Bhogaraju *et al.*, Phosphoribosylation of Ubiquitin Promotes Serine Ubiquitination and Impairs Conventional Ubiquitination. *Cell* **167**, 1636-1649 e1613 (2016).
24. M. Wan *et al.*, Deubiquitination of phosphoribosyl-ubiquitin conjugates by phosphodiesterase-domain-containing *Legionella* effectors. *Proc Natl Acad Sci U S A* **116**, 23518-23526 (2019).
25. D. Shin *et al.*, Regulation of Phosphoribosyl-Linked Serine Ubiquitination by Deubiquitinases DupA and DupB. *Mol Cell* **77**, 164-179 e166 (2020).
26. K. C. Jeong, J. A. Sexton, J. P. Vogel, Spatiotemporal regulation of a *Legionella pneumophila* T4SS substrate by the metaeffector SidJ. *PLoS Pathog* **11**, e1004695 (2015).
27. J. Qiu *et al.*, A unique deubiquitinase that deconjugates phosphoribosyl-linked protein ubiquitination. *Cell Res* **27**, 865-881 (2017).
28. S. Bhogaraju *et al.*, Inhibition of bacterial ubiquitin ligases by SidJ-calmodulin catalysed glutamylation. *Nature* **572**, 382-386 (2019).
29. J. C. Havey, C. R. Roy, Toxicity and SidJ-Mediated Suppression of Toxicity Require Distinct Regions in the SidE Family of *Legionella pneumophila* Effectors. *Infect Immun* **83**, 3506-3514 (2015).
30. R. K. Laguna, E. A. Creasey, Z. Li, N. Valtz, R. R. Isberg, A *Legionella pneumophila*-translocated substrate that is required for growth within macrophages and protection from host cell death. *Proc Natl Acad Sci U S A* **103**, 18745-18750 (2006).
31. E. A. Creasey, R. R. Isberg, The protein SdhA maintains the integrity of the *Legionella*-containing vacuole. *Proc Natl Acad Sci U S A* **109**, 3481-3486 (2012).
32. W. Y. Choi *et al.*, SdhA blocks disruption of the *Legionella*-containing vacuole by hijacking the OCRL phosphatase. *Cell Rep* **37**, 109894 (2021).
33. S. Sharma, A. Skowronek, K. S. Erdmann, The role of the Lowe syndrome protein OCRL in the endocytic pathway. *Biol Chem* **396**, 1293-1300 (2015).
34. M. A. De Matteis, L. Staiano, F. Emma, O. Devuyst, The 5-phosphatase OCRL in Lowe syndrome and Dent disease 2. *Nat Rev Nephrol* **13**, 455-470 (2017).
35. D. M. Pilla *et al.*, Guanylate binding proteins promote caspase-11-dependent pyroptosis in response to cytoplasmic LPS. *Proc Natl Acad Sci U S A* **111**, 6046-6051 (2014).
36. B. C. Liu *et al.*, Constitutive Interferon Maintains GBP Expression Required for Release of Bacterial Components Upstream of Pyroptosis and Anti-DNA Responses. *Cell Rep* **24**, 155-168 e155 (2018).
37. I. S. Anand, W. Choi, R. R. Isberg, Components of the endocytic and recycling trafficking pathways interfere with the integrity of the *Legionella*-containing vacuole. *Cell Microbiol* **22**, e13151 (2020).

38. M. N. Seaman, Cargo-selective endosomal sorting for retrieval to the Golgi requires retromer. *J Cell Biol* **165**, 111-122 (2004).
39. C. Burd, P. J. Cullen, Retromer: a master conductor of endosome sorting. *Cold Spring Harb Perspect Biol* **6** (2014).
40. I. Finsel *et al.*, The *Legionella* effector RidL inhibits retrograde trafficking to promote intracellular replication. *Cell Host Microbe* **14**, 38-50 (2013).
41. K. Barlocher *et al.*, Structural insights into *Legionella* RidL-Vps29 retromer subunit interaction reveal displacement of the regulator TBC1D5. *Nature Communications* **8** (2017).
42. K. H. Berger, R. R. Isberg, Two distinct defects in intracellular growth complemented by a single genetic locus in *Legionella pneumophila*. *Mol Microbiol* **7**, 7-19 (1993).
43. J. M. Park, S. Ghosh, T. J. O'Connor, Combinatorial selection in amoebal hosts drives the evolution of the human pathogen *Legionella pneumophila*. *Nat Microbiol* **5**, 599-609 (2020).
44. E. Geisinger *et al.*, Antibiotic susceptibility signatures identify potential antimicrobial targets in the *Acinetobacter baumannii* cell envelope. *Nat Commun* **11**, 4522 (2020).
45. K. M. McCoy, M. L. Antonio, T. van Opijnen, MAGenTA: a Galaxy implemented tool for complete Tn-Seq analysis and data visualization. *Bioinformatics* **33**, 2781-2783 (2017).
46. T. van Opijnen, K. L. Bodi, A. Camilli, Tn-seq: high-throughput parallel sequencing for fitness and genetic interaction studies in microorganisms. *Nat Methods* **6**, 767-772 (2009).
47. J. J. Merriam, R. Mathur, R. Maxfield-Boumil, R. R. Isberg, Analysis of the *Legionella pneumophila* fliI gene: intracellular growth of a defined mutant defective for flagellum biosynthesis. *Infect Immun* **65**, 2497-2501 (1997).
48. A. D. Hempstead, R. R. Isberg, Inhibition of host cell translation elongation by *Legionella pneumophila* blocks the host cell unfolded protein response. *Proc Natl Acad Sci U S A* **112**, E6790-6797 (2015).
49. V. P. Losick, E. Haenssler, M. Y. Moy, R. R. Isberg, LnaB: a *Legionella pneumophila* activator of NF-kappaB. *Cell Microbiol* **12**, 1083-1097 (2010).
50. K. C. Barry, N. T. Ingolia, R. E. Vance, Global analysis of gene expression reveals mRNA superinduction is required for the inducible immune response to a bacterial pathogen. *Elife* **6** (2017).
51. J. P. Bardill, J. L. Miller, J. P. Vogel, IcmS-dependent translocation of SdeA into macrophages by the *Legionella pneumophila* type IV secretion system. *Mol Microbiol* **56**, 90-103 (2005).
52. D. J. Lampe, M. E. Churchill, H. M. Robertson, A purified mariner transposase is sufficient to mediate transposition in vitro. *EMBO J* **15**, 5470-5479 (1996).
53. B. Byrne, M. S. Swanson, Expression of *Legionella pneumophila* virulence traits in response to growth conditions. *Infect Immun* **66**, 3029-3034 (1998).
54. G. M. Conover, I. Derre, J. P. Vogel, R. R. Isberg, The *Legionella pneumophila* LidA protein: a translocated substrate of the Dot/Icm system associated with maintenance of bacterial integrity. *Mol Microbiol* **48**, 305-321 (2003).
55. T. J. O'Connor, Y. Adepoju, D. Boyd, R. R. Isberg, Minimization of the *Legionella pneumophila* genome reveals chromosomal regions involved in host range expansion. *Proc Natl Acad Sci U S A* **108**, 14733-14740 (2011).

762 56. S. R. Shames *et al.*, Multiple *Legionella pneumophila* effector virulence phenotypes
763 revealed through high-throughput analysis of targeted mutant libraries. *Proc Natl Acad*
764 *Sci U S A* **114**, E10446-E10454 (2017).
765 57. D. T. Isaac, R. K. Laguna, N. Valtz, R. R. Isberg, MavN is a *Legionella pneumophila*
766 vacuole-associated protein required for efficient iron acquisition during intracellular
767 growth. *Proc Natl Acad Sci U S A* **112**, E5208-5217 (2015).
768 58. M. Romano-Moreno *et al.*, Molecular mechanism for the subversion of the retromer coat
769 by the *Legionella* effector RidL. *Proc Natl Acad Sci U S A* **114**, E11151-E11160 (2017).
770 59. K. McGourty *et al.*, Salmonella inhibits retrograde trafficking of mannose-6-phosphate
771 receptors and lysosome function. *Science* **338**, 963-967 (2012).
772 60. A. H. Gaspar, M. P. Machner, VipD is a Rab5-activated phospholipase A1 that protects
773 *Legionella pneumophila* from endosomal fusion. *Proc Natl Acad Sci U S A* **111**, 4560-
774 4565 (2014).
775 61. B. Ku *et al.*, VipD of *Legionella pneumophila* targets activated Rab5 and Rab22 to
776 interfere with endosomal trafficking in macrophages. *PLoS Pathog* **8**, e1003082 (2012).
777 62. M. Mari *et al.*, SNX1 defines an early endosomal recycling exit for sortilin and mannose
778 6-phosphate receptors. *Traffic* **9**, 380-393 (2008).
779 63. I. Anand, W. Choi, R. R. Isberg, The vacuole guard hypothesis: how intravacuolar
780 pathogens fight to maintain the integrity of their beloved home. *Curr Opin Microbiol* **54**,
781 51-58 (2020).
782 64. C. R. Beuzon *et al.*, *Salmonella* maintains the integrity of its intracellular vacuole through
783 the action of SifA. *EMBO J* **19**, 3235-3249 (2000).
784 65. C. A. Elwell *et al.*, *Chlamydia trachomatis* co-opts GBF1 and CERT to acquire host
785 sphingomyelin for distinct roles during intracellular development. *PLoS Pathog* **7**,
786 e1002198 (2011).
787 66. C. van Ooij *et al.*, Host cell-derived sphingolipids are required for the intracellular
788 growth of *Chlamydia trachomatis*. *Cell Microbiol* **2**, 627-637 (2000).
789 67. N. Mellouk *et al.*, *Shigella* subverts the host recycling compartment to rupture its vacuole.
790 *Cell Host Microbe* **16**, 517-530 (2014).
791 68. J. Ruiz-Albert *et al.*, Complementary activities of SseJ and SifA regulate dynamics of the
792 *Salmonella typhimurium* vacuolar membrane. *Mol Microbiol* **44**, 645-661 (2002).
793 69. X. Li, D. E. Anderson, Y. Y. Chang, M. Jarnik, M. P. Machner, VpdC is a ubiquitin-
794 activated phospholipase effector that regulates *Legionella* vacuole expansion during
795 infection. *Proc Natl Acad Sci U S A* **119**, e2209149119 (2022).
796 70. M. Zhang *et al.*, Members of the *Legionella pneumophila* Sde family target tyrosine
797 residues for phosphoribosyl-linked ubiquitination. *RSC Chem Biol* **2**, 1509-1519 (2021).
798 71. Y. Abu Kwaik, The phagosome containing *Legionella pneumophila* within the protozoan
799 *Hartmannella vermiformis* is surrounded by the rough endoplasmic reticulum. *Appl*
800 *Environ Microbiol* **62**, 2022-2028 (1996).
801 72. Y. Liu, Z. Q. Luo, The *Legionella pneumophila* effector SidJ is required for efficient
802 recruitment of endoplasmic reticulum proteins to the bacterial phagosome. *Infect Immun*
803 **75**, 592-603 (2007).
804 73. B. Iglewicz, D. C. Hoaglin, *How to detect and handle outliers*, ASQC basic references in
805 quality control (ASQC Quality Press, Milwaukee, Wis., 1993), pp. ix, 87 p.
806 74. Y. Benjamini, A. M. Krieger, D. Yekutieli, Adaptive linear step-up procedures that
807 control the false discovery rate. *Biometrika* **93**, 491-507 (2006).

808

809

810

811

812

813

814 **Figure legends**

815 **Fig. 1. Tn-seq identifies mutations that aggravate loss of Sde function.**

816 (**A**) Schematic view of Tn-seq analysis to identify aggravating mutations. *Himar-1* pools were
817 constructed in parallel in SK01 (WT) and SK02 (Δ*sde*) strains and insertion site abundance was
818 determined after growth in broth (Materials and Methods). Three of the sequenced pools were
819 incubated with BMDMs for 24 hrs in parallel, plated on bacteriological medium, and relative
820 abundance of insertions was determined by HTS to determine fitness of individual mutations in
821 the two different strain backgrounds (Materials and Methods). (**B, C**) Volcano plots of the
822 relative fitness, represented as modified Z scores (Materials and Methods) comparing replication
823 in BMDM versus AYE for either WT or Δ*sde* strains. Candidates were identified based on
824 criteria of $Z_{MOD} > 2$ from the population median and were statistically significant ($p < 0.05$)
825 based on unpaired t-test after Two-stage step-up correction (indicated by dotted red line) (73, 74).
826 Blue font indicates IDTS that are the focus of study or which were previously shown to have an
827 intracellular growth defect. (D) Volcano plots displaying relative fitness of insertion mutations in
828 a Δ*sde* background compared to the WT background for intracellular growth in BMDM. Genes
829 were identified as candidates based > 1 MAD from the population mean and statistical
830 significance ($p < 0.05$) based on unpaired t-test after Two-stage step-up correction method (74)
831 (indicated by dotted line). Data are based on n=3 biological replicates of pools made in each
832 strain. (E) Volcano plots of relative fitness (modified Z scores) of mutations in Δ*sde* background
833 versus WT background for growth in AYE broth culture. Grey, blue and red squares represent
834 whole genes, *icm/dot* or Icm/Dot translocated substrate (IDTS) genes and genes selected based
835 on the following criteria, respectively. Criteria: 1) mutations who showed fitness differences
836 (Δ*sde* - WT) > 1 median absolute deviation (MAD) from the population median fitness and were

837 statistically significant based on unpaired t tests ($p < 0.05$; Dataset S1), 2) genes that were
838 *Icm/Dot* translocated substrates, and 3) genes possibly involved in LCV biogenesis.
839
840 **Fig. 2. Identification of mutations that aggravate the intracellular growth defect of Δ*sde*.**
841 (A-C) BMDMs were challenged with WT (Lp02) or noted *L. pneumophila* mutants expressing
842 luciferase (P*ahpC*::lux). Intracellular growth was determined by measuring luminescence hourly.
843 Data shown and error bars are mean ± SEM at 12 hr increments (mean of 3 technical replicates
844 and a representative of 3 biological replicates).
845
846 **Fig. 3. Aggravating mutations result in loss of LCV integrity and accelerated pyroptotic**
847 **cell death at early infection times.**
848 (A) Examples of cytosolic and vacuolar bacteria. Macrophages were challenged with either WT
849 or noted mutant strains for 2 hr, fixed, probed with anti-*L. pneumophila* (Alexa Fluor 594
850 secondary, red), permeabilized, and reprobed with anti-*L. pneumophila* (Alexa Fluor 488
851 secondary, green). Cytosolic bacteria are accessible to both antibodies, shown in yellow in the
852 merged image, whereas vacuolar bacteria are shown in green. The scale bar represents 10 μm. (B)
853 Disrupted vacuole integrity of *L. pneumophila* strains at 2 hr post-infection. BMDMs were
854 challenged with indicated strains, fixed and stained for bacteria before and after permeabilization.
855 For quantification, bacteria that stained positively in the absence of permeabilization were
856 divided by the total infected population (mean ± SEM; three biological replicates with 300 LCVs
857 were counted per replicate) (C) Kinetics of macrophage cell death, with infection of indicated
858 strains. BMDMs were infected with *L. pneumophila* WT or mutant strains and propidium iodide
859 (PI) incorporation was used to monitor cell death. Data shown and error bars are mean ± SEM

for 30 min increments and a representative of 3 biological replicates. Statistical analysis was performed using one-way ANOVA with Tukey's multiple comparisons, with significance represented as: *p<0.05; ****p < 0.0001.

Fig. 4. Increased aggregation of RTN4 is associated with maintenance of LCV integrity. (A) Vacuole integrity of *L. pneumophila* strains at 2 hr post-infection. BMDMs were challenged with indicated strains, fixed and stained for bacteria before and after permeabilization. The percentages of cytosolic bacteria were calculated. Data displayed as mean ± SEM for three biological replicates. (B) Complementation of Δ*sdhA*Δ*sde* strain *in trans*. Shown is aggregation of RTN4 in fixed samples of BMDM challenged with *L. pneumophila* Δ*sdhA*Δ*sde* harboring p*sdeA*. Bacteria and RTN4 were probed as described (Materials and Methods), scale bar 10 μm. (C) Vacuole integrity of *L. pneumophila* strains at 4 hr post-infection. Data shown as mean ± SEM for four biological replicates. At least 70 LCVs were counted per replicate (A, C). Statistical significance was tested using one-way ANOVA with Tukey's multiple comparisons; *p<0.05,**p<0.01, ***p<0.001 (A, C). (D) A Representative micrograph of RTN4 associated with individual LCVs, scale bar 10 μm. (E) Quantification of RTN4 intensity associated with individual LCVs. Loss of SidJ results in increased association of RTN4 about LCV. Images of individual LCVs were captured and pixel intensities of RTN4 staining about regions of interest were determined. More than 70 LCVs were quantified per experiment and data were pooled from 3 biological replicates (**p<0.01; Mann-Whitney test)

Fig. 5. Interference with host endocytic and retromer-mediated trafficking pathways allows partial rescue of vacuole integrity defect.

(A) Effect of si-Rab5B on vacuole integrity. Left: immunoblot of SDS-polyacrylamide gel probed with anti-Rab5B after depletion with si-Rab5B or control scrambled si-RNA. Right: the percentage of cytosolic bacteria from BMDMs treated with si-Control or si-Rab5B, and challenged with noted *L. pneumophila* strains for 2 hrs, followed by probing as described (Materials and Methods). (B) Effect of si-SNX1 on vacuole integrity. Left: immunoblot of SDS-polyacrylamide gel probed with anti-SNX1 after depletion with si-SNX1 or control scrambled si-RNA. Right: the percentage of cytosolic bacteria from BMDMs treated with si-Control or si-SNX1 and challenged with noted *L. pneumophila* strains for 2 hrs, followed by probing as described (Materials and Methods). For immunoblotting, β-actin was used as loading control. The data shown are mean ± SEM, using three biological replicates, with at least 100 LCVs counted per biological replicate. Statistical analysis was conducted using unpaired two-tailed Student's t test and significance displayed as $**p < 0.01$ or $****p < 0.0001$.

Fig. 6. Transcription of *sde* genes is downregulated during *L. pneumophila* infection of BMDMs.

Transcript abundance of indicated genes was determined during infection. PMA-differentiated U937 cells were challenged with *L. pneumophila* WT and RNA was extracted at the noted time points. Transcripts were normalized to 16s rRNA, and then displayed relative to transcription level measured at 1hr post-infection and represented as fold change.

Fig. 7. Schematic model of how *Legionella* combats vacuole disruption in a temporally-regulated process.

Soon after internalization, the *Legionella*-containing vacuole is walled off with RTN4-rich tubular ER aggregates as a consequence of PR ubiquitination on RTN4 by Sde proteins (22) **[Step 1. Walled off]**. At early time of infection, the barrier as well as SdhA and RidL (backup vacuole guards in case the barrier is breached) protects the LCV from host membrane traffic derived from the early endosome. Over time, the wall is breached as the aggregates are dissipated by SidJ, a metaeffector that inactivates Sde proteins, (26-29) and Dups (DupA and DupB), enzymes that deubiquitinate PR-Ub-linked substrates (24, 25) **[Step 2. Wall Breaks Down]**. When the barrier around the LCV is dismantled, SdhA and RidL act to divert and inactivate disruptive compartments derived from the early/recycling endosomes to allow the LCV to be replication-permissive (32, 37) **[Step 3. Vacuole guards]**.

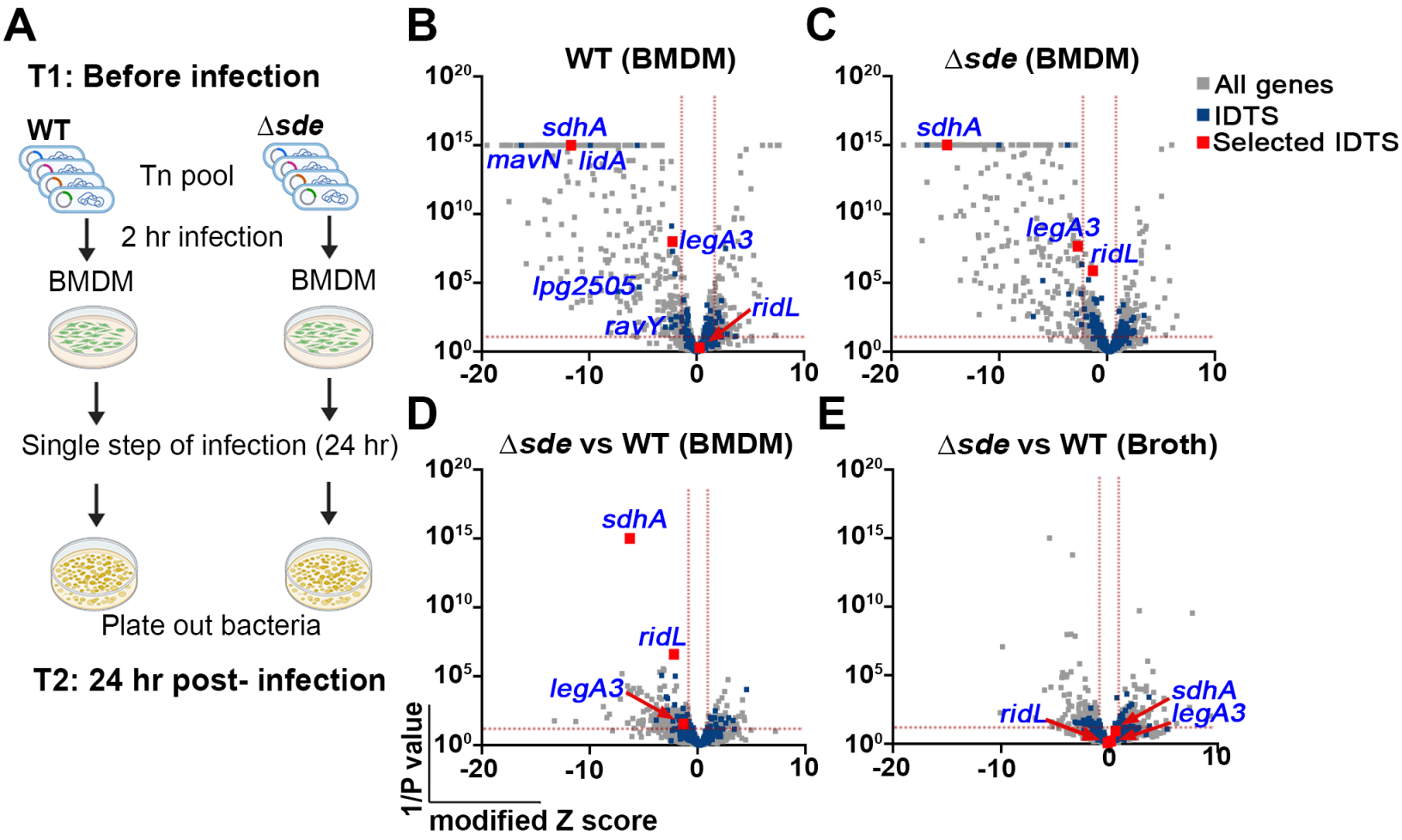

Figure 1

A

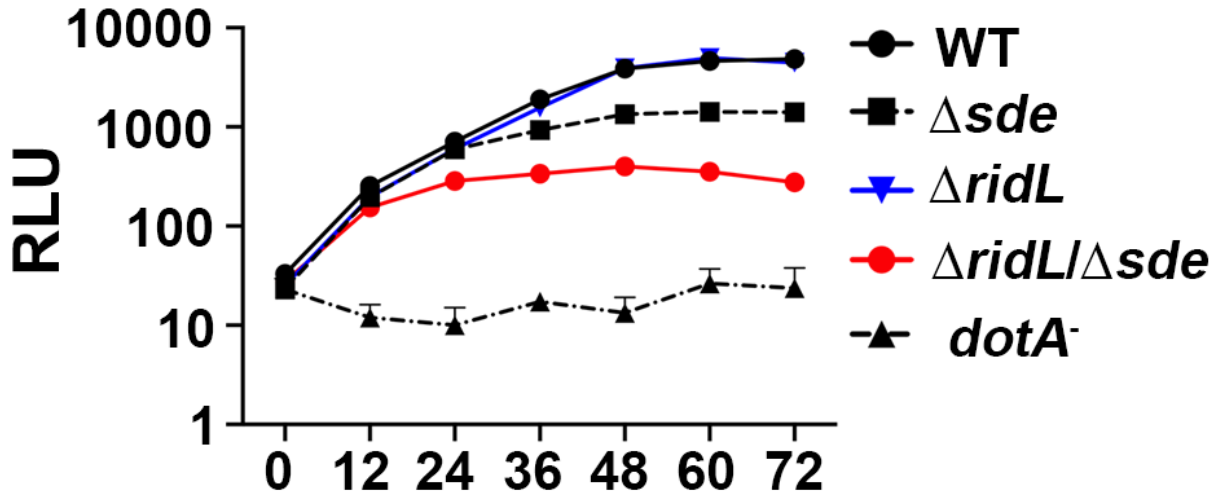

B

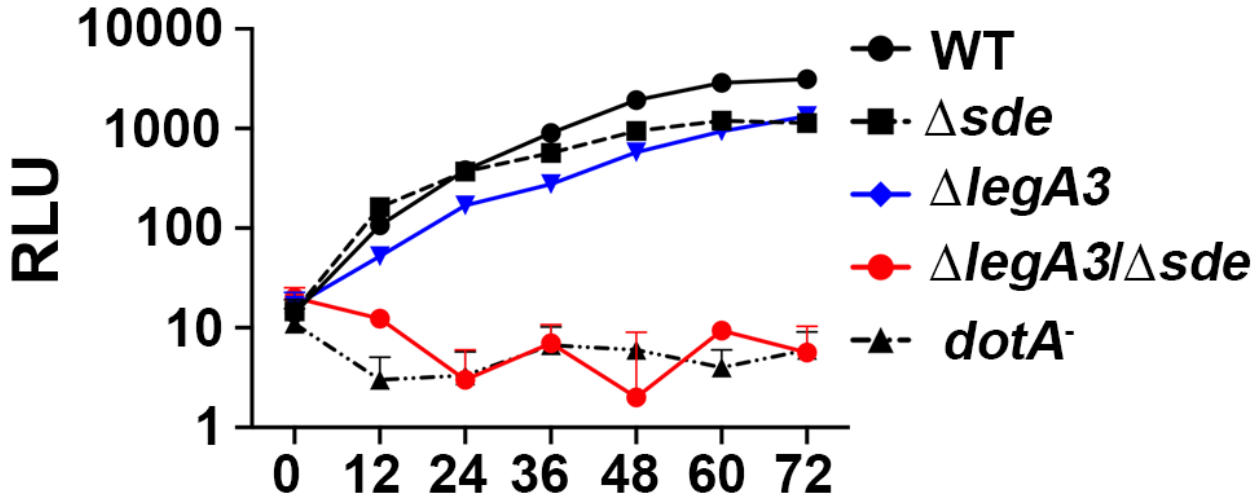

C

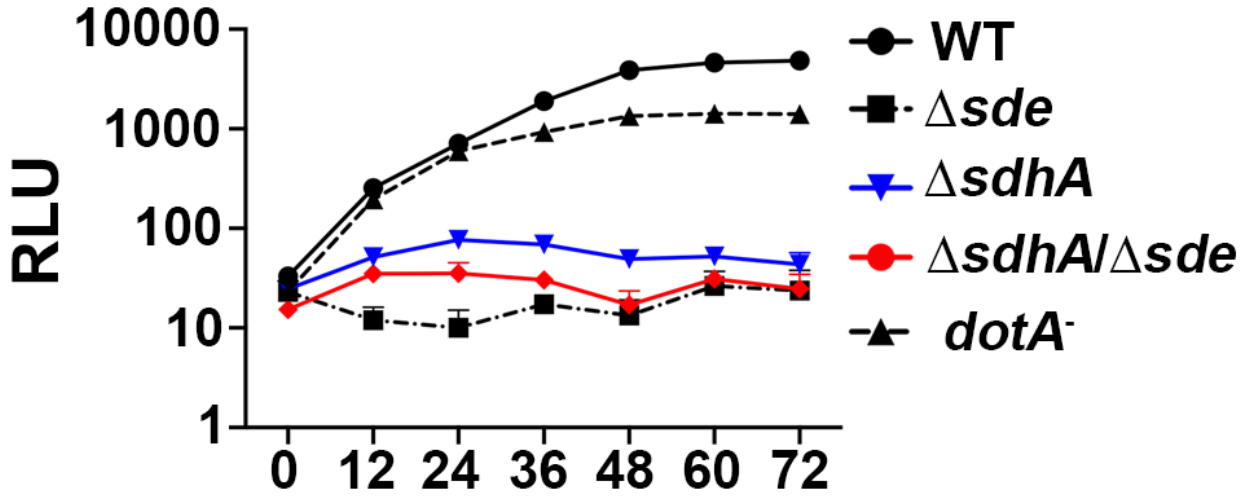

Figure 2

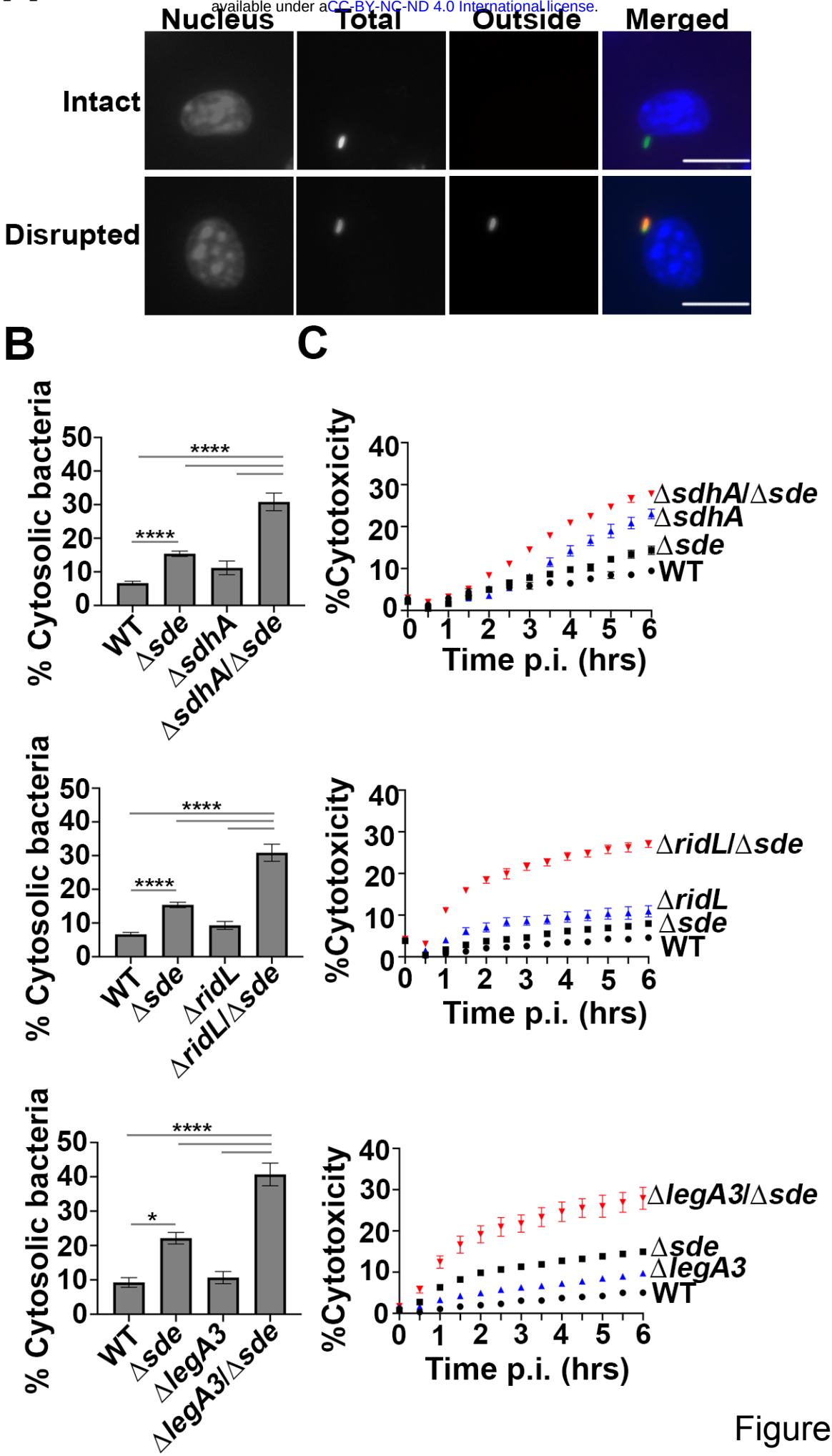

Figure 3

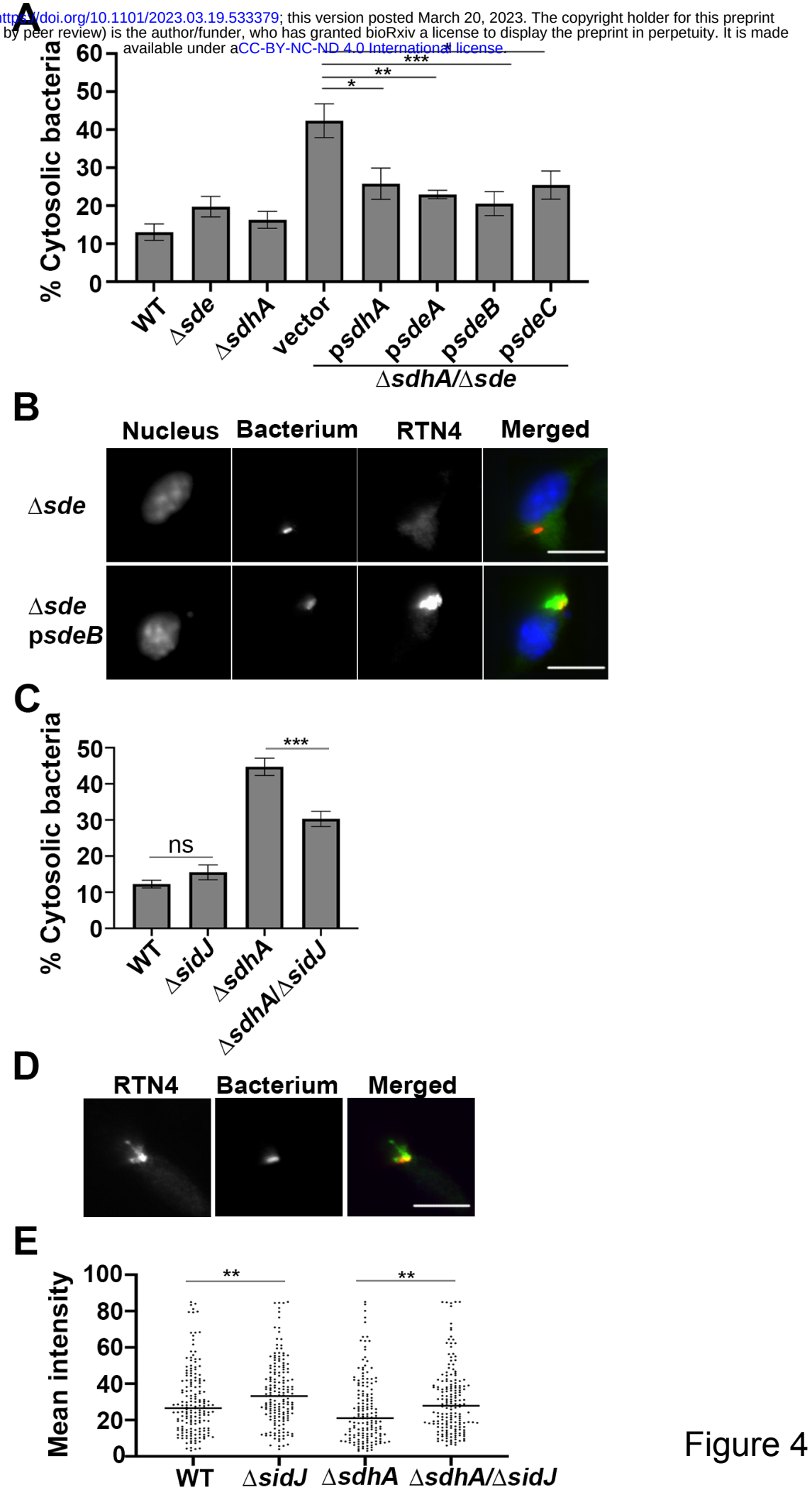

Figure 4

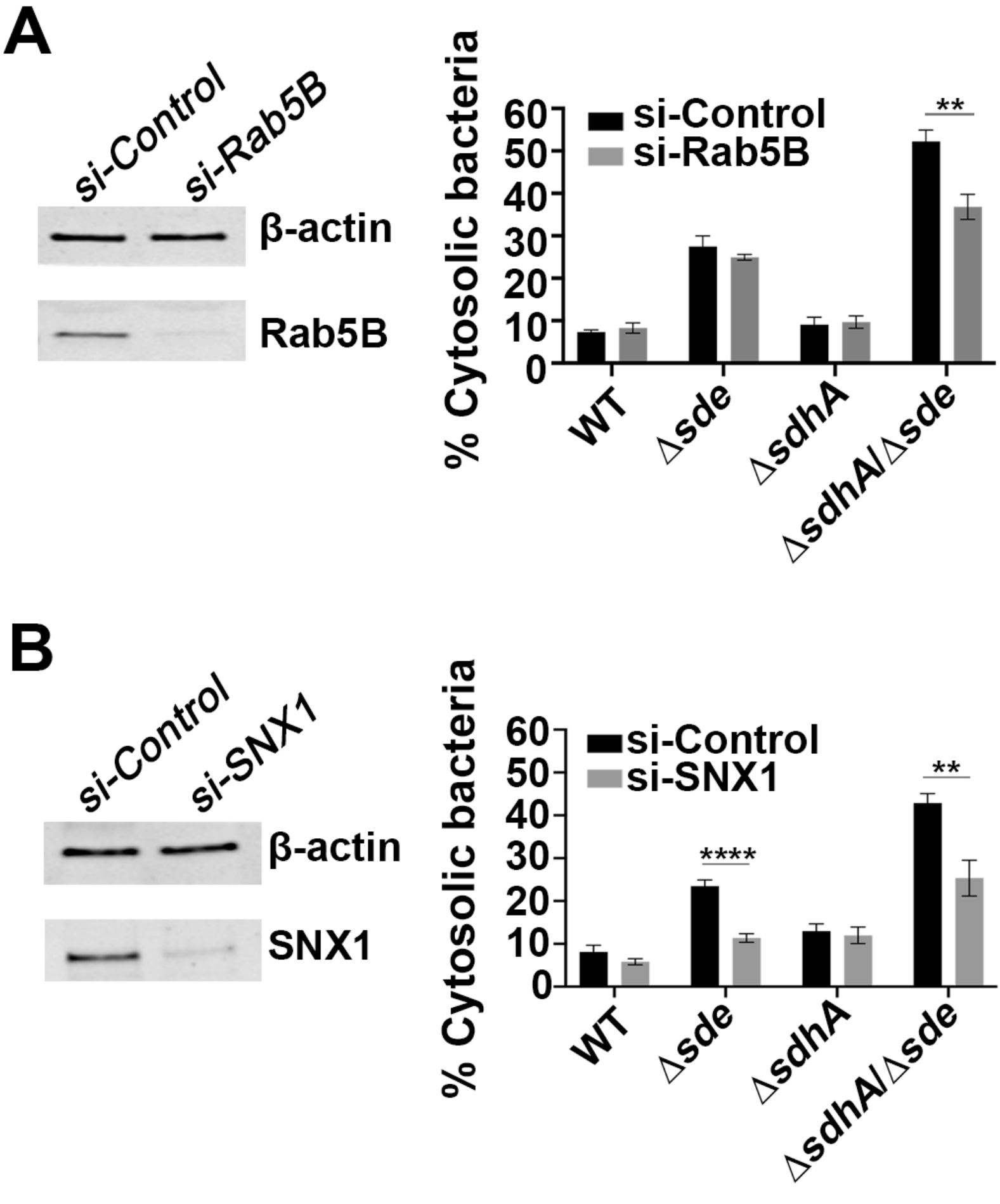

Figure 5

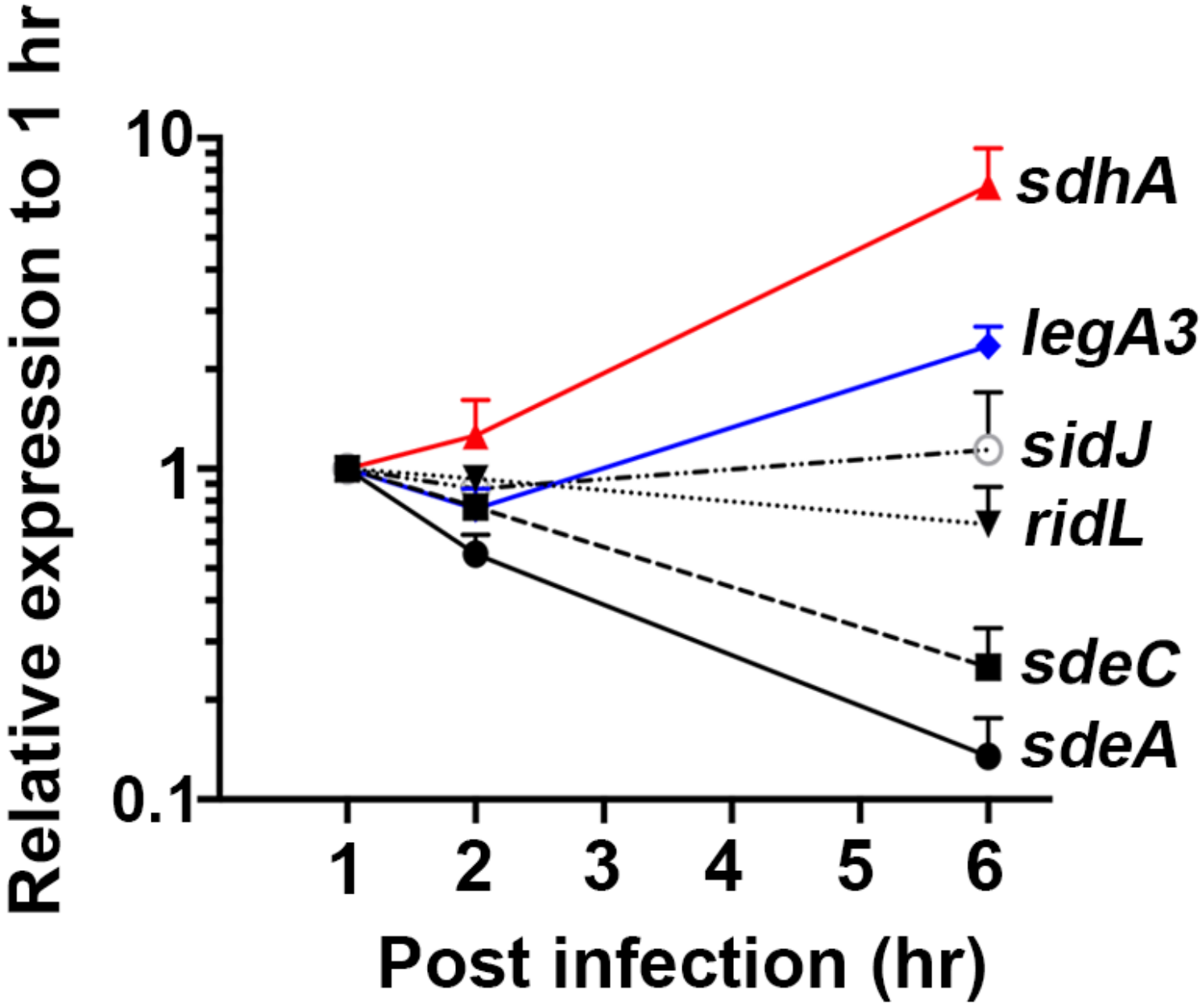

Figure 6

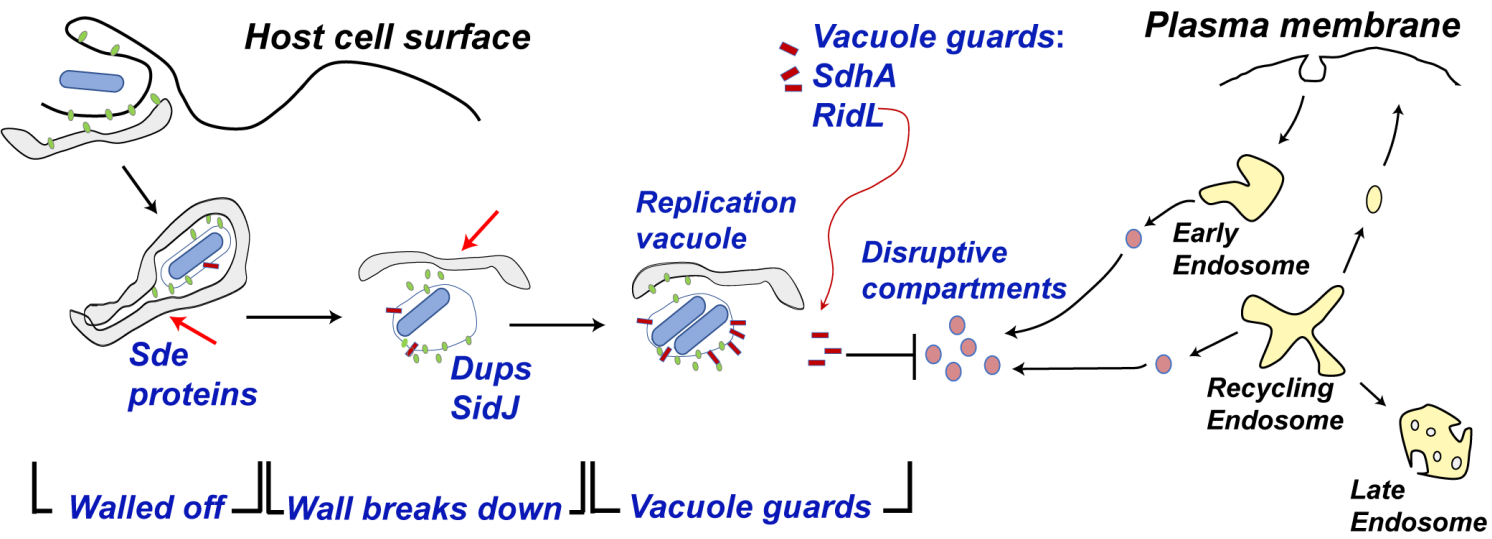

Figure 7

Supporting Information

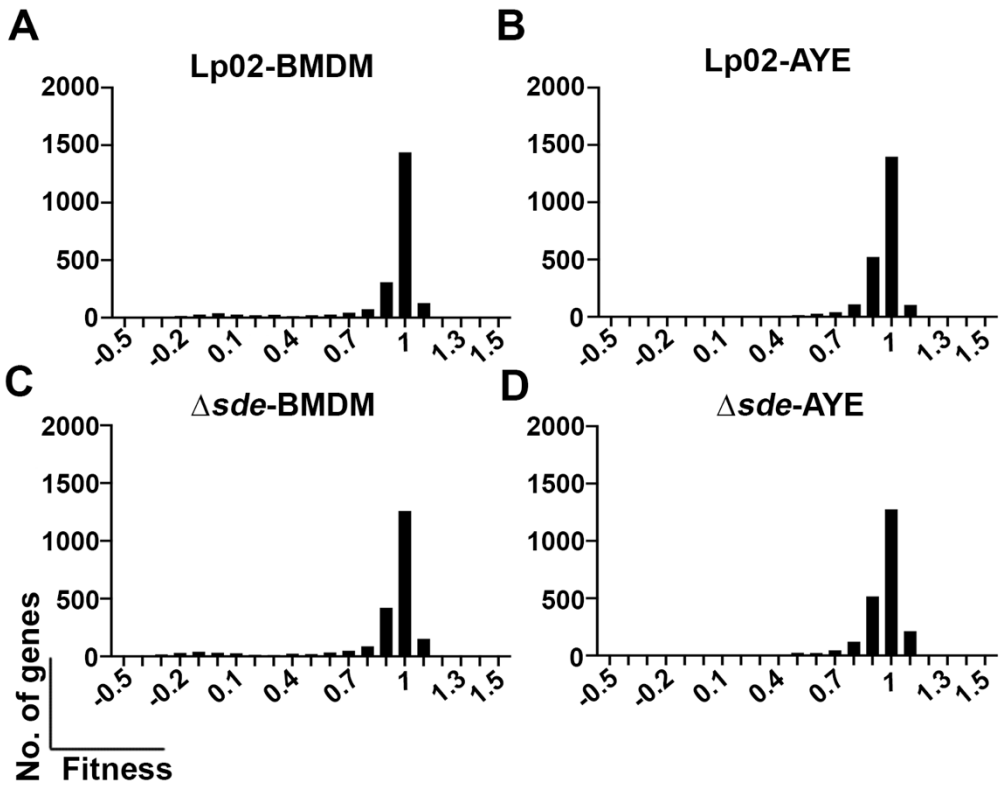

Fig. S1 (Linked to Fig.1). Histogram plots of fitness for all *L. pneumophila* genes represented on Tn-seq.

Histogram of WT (SK01) Tn-seq pool following either infection in BMDM (A) or growth in nutrient-rich AYE medium (B). Histogram of Δ*sde* (SK02) Tn-seq pool following infection in BMDM (C) or growth in nutrient-rich AYE medium (D).

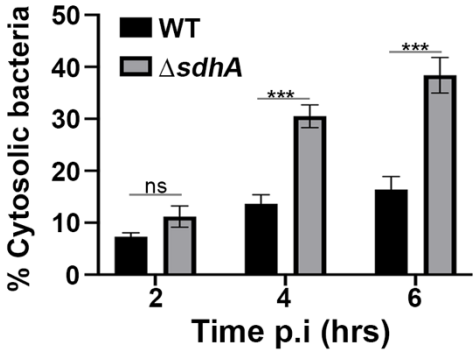

Fig. S2 (Linked to Fig.3). The integrity of LCVs harboring Δ*sdhA* strains after challenge with *L. pneumophila*.

Percent cytosolic bacteria was quantified based on antibody accessibility. BMDMs were infected with either WT or Δ*sdhA* strains for 2, 4, and 6 hr, fixed, and stained with antibodies. The internalized bacteria in the absence of permeabilization were calculated relative to the total infected population (mean ± SEM; three biological replicates were performed and 100 LCVs were counted per biological replicate). Statistical analysis was conducted using unpaired two-tailed Student's t test (ns, not significant; ***$p < 0.001$).

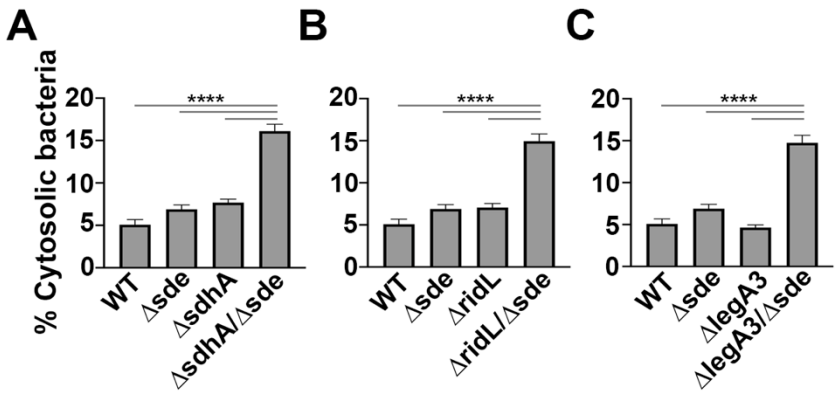

Fig. S3 (Linked to Fig. 3). The loss of *sdhA*, *ridL* and *legA3* aggravated vacuole disruption in Δ*sde* strain.

Vacuole integrity was measured based on antibody accessibility. BMDMs in a 96 well plate were infected with the indicated strains for 2 hr, fixed and stained with antibodies. The images were taken by Lionheart automatic microscope using 10X magnification objective. The internalized bacteria in the absence of permeabilization were calculated relative to total infected population to determine fraction of disrupted vacuoles (mean ± SEM; three biological replicates were performed and 1000-3000 LCVs were counted per biological replicate). Statistical significance was tested using one-way ANOVA with Tukey's multiple comparisons; ***p <0.001.

Table S1. Strains, Plasmids and Oligonucleotides used in this study

Strains

Name	Genotype	Description	Reference
L.pneumophila			
Lp02	Philadelphia 1 *thyA*$^{-}$ *rpsL hsdR*	Wild type strain	(1)
SK01	Lp02 *thyA*$^{+}$	Wild type strain *thyA*$^{+}$	This work
Lp03	*thyA*$^{+}$ *rpsL hsdR dotA03*	Icm/Dot translocation deficient	(1)
JV6113	Lp02 Δ*sidE* Δ*sdeC* Δ*sdeBA* (Δ*lpg0234* Δ*lpg2153* Δlpg*2156-2157*)	*sidE* family deletion mutant	(2)
SK02	JV6113 *thyA*$^{+}$	JV6113 strain *thyA*$^{+}$	This work
SK03	Lp02 *thyA*$^{+}$Δ*sdhA*	*sdhA* deletion mutant	This work
SK04	JV6113 *thyA*$^{+}$ Δ*sdhA*	*sdhAsidE* family deletion mutant	This work
SK05	Lp02 *thyA*$^{+}$ Δ*ridL*	*ridL* deletion mutant	This work
SK06	JV6113 *thyA*$^{+}$ Δ*ridL*	*ridLsidE* family deletion mutant	This work
SK07	Lp02 *thyA*$^{+}$ Δ*legA3*	*legA3* deletion mutant	This work
SK08	JV6113 *thyA*$^{+}$ Δ*legA3*	*legA3sidE* family deletion mutant	This work
SK09	Lp02 *thyA*$^{+}$ Δ*sdhA* Δ*ridL*	*sdhAridL* deletion mutant	This work
SK10	Lp02 *thyA*$^{+}$ Δ*sdhA* Δ*legA3*	*sdhA legA3* deletion mutant	This work
SK11	Lp02 *thyA*$^{+}$ Δ*ridL* Δ*legA3*	*ridL legA3* deletion mutant	This work
SK12	Lp02 *thyA*$^{+}$ *kan*^{R} P_{ahpc}::*lux*	wild type strain Lux^{+}	This work
SK13	JV6113 *thyA*$^{+}$ *kan*^{R} P_{ahpc}::*lux*	*sidE* family deletion mutant Lux^{+}	This work
SK14	SK02 *kan*^{R} P_{ahpc}::*lux*	*sdhA* deletion mutant Lux^{+}	This work
SK15	SK03 *kan*^{R} P_{ahpc}::*lux*	*sdhAsidE* family deletion mutant Lux^{+}	This work
SK16	SK04 *kan*^{R} P_{ahpc}::*lux*	*ridL* deletion mutant Lux^{+}	This work
SK17	SK05 *kan*^{R} P_{ahpc}::*lux*	*ridLsidE* family deletion mutant	This work
SK18	SK06 *kan*^{R} P_{ahpc}::*lux*	*legA3* deletion mutant Lux^{+}	This work
SK19	SK07 *kan*^{R} P_{ahpc}::*lux*	*legA3 sidE* family deletion mutant Lux^{+}	This work
Lp03 lux^{+}	Lp03 *kan*^{R} P_{ahpc}::*lux*	Icm/Dot translocation deficient Lux^{+}	(3)
JV4487	Δ*sidJ*	*sidJ* deletion mutant	(2)
SK20	Lp02 Δ*sdhA*	*sdhA* deletion mutant	This work
SK21	Lp02 Δ*sdhA* Δ*sidJ*	*sdhAsidJ* deletion mutant	This work
SK22	SK01+ pMMB207Δ267		This work
SK23	SK02+ pMMB207Δ267		This work
SK24	SK03+ pMMB207Δ267		This work
SK25	SK04+ pMMB207Δ267		This work

Plasmids

Name	Features	Description	Reference
pTO100MmeI	R6K*ori kan*^{R}, *sacB*, *ampR*, *himar1*-MmeI, C9 transposase	Tn-seq transposon mutagenesis plasmid	(5)
pSR47S	R6K*ori sacB*, *kan*^{R}	suicide vector	(6)
pSR47S-P_{ahpc}::lux	R6K*ori sacB*, *kan*^{R} P_{ahpc}::lux	pSR47 containing *P. luminescens* lux operon	(7)
pJB3395	pBluescript*::thyA*$^+$ *amp*^{R}	*thyA* allelic exchange vector	J. Vogel
pTO243	pbluescript:: PolyHis-*attR1*-[*Kan*^{R}-*Kan*^{R}- *ccdB*]-*attR2*		O'Connor Tamara
pSK01	pSR47S:: Δ*sdhA*	*sdhA* deletion plasmid	
pSK02	pSR47S:: Δ*ridL*	*ridL* deletion plasmid	
pMMB207	*OriR* (RSF1010), Cm^R		(8)
pMMB207Δ267	*OriR* (RSF1010), Cm^R, Δ267	pMMB207 lacking 267 bps of N- terminal *mobA*	Elizabeth Creasey
pSK03	pMMB207Δ267::PolyHis-*attR1*-[*Kan*^{R}-*Kan*^{R}-*ccdB*]-*attR2*	Gateway destination version of pMMB207Δ267	This work
pSK04	pMMB207Δ267::PolyHis-*attB1*-*sdeA*-*attB2*	*sdeA* complementation plasmid	This work
pSK05	pMMB207Δ267::PolyHis-*attB1*-*sdeB*-*attB2*	*sdeB* complementation plasmid	This work
pSK06	pMMB207Δ267::PolyHis-*attB1*-*sdeC*-*attB2*	*sdeC* complementation plasmid	This work
pTO198	pSR47S::Δ*legA3*	*legA3* deletion plasmid	(9)

E. coli

DH5α	*supE44 ΔlacU169*(*Φ80lacZDM15*) *hsdR17 recA1 endA1 gyrA96 thi-1 relA1*	
DH5α λpir	DH5α (λ*pir*) *tet*::Mu recA	(12)
BL21 DE3	F$^+$ *ompT hsdSB dcm* (*DE3*)	

Oligonucleotides

Name	Sequences (5' to 3')
Construction of sdhA mutant	
SK1	GGCGCTAATTGCTGAAATCATTTCAATATTAAAAAAATTAAC
SK2	CCGGGGGATGAACAATTTACCCCCTG
SK3	GATTTCAGCAATTAGCGCCATCCGCATAAAAATATTTG
SK4	GAACTAGGGCGTAGGCGTTGACCATTAAAAG
pSR47s_sdhA_F	TTGTTCATCCCCCGGGCTGCAGGAAT
pSR47s_sdhA_R	CCTACGCCCTAGTTCTAGAGCGGCCGCC
Construction of ridL mutant	
SK5	TCATTATTATTATGTGTTCATTTTAAGCCAAAAAAC

SK6	AGCCCGGGGGGTTATTACTGAAGTCGTGAC
SK7	CTAGAACTAGGATACTGGTGGATTGTCG
SK8	TGAACACATAATAATAATGACTTTGGCTCTC
pSR47s_ridL_F	CAGTAATAACCCCCCGGGCTGCAGGAAT
pSR47s_ridL_R	CACCAGTATCCTAGTTCTAGAGCGGCCGCC

Confirmation of recombinant plasmid

pSR47s_conF	GGGAACAAAAGCTGGAGC
pSR47s_conR	GTGAACGGCAGGTATATGT

qRT-PCR

Name	Sequences (5’ to 3’)
rRNA_F	AGAGATGCATTAGTGCCTTCGGGA
rRNA_R	ACTAAGGATAAGGGTTGCGCTCGT
ridL_F	GTCCTCTGAAGGATAGCGAAAC
ridL_R	GTGTAAGTTCCCGCAACAAATC
sidE_F	GCCTAAGTACGTTGAAGGGATAG
sidE_R	GCCTGTCAAGAGCACCTTTA
sdeC_F	AAATCAGGAGAAGCGGTTAGG
sdeC_R	CGTGAGAGCCGGGATAATTT
sdeB_F	CCAGGCTTCACTCACTTGATAA
sdeB_R	CCTCTCGATACCTACTGTGTCT
sdeA_F	CCCACTGCACCACAAGATAA
sdeA_R	GGTATACGGTTTGCCCAGATAG
sdhA_F	GGAAGGCAGGATTCTCCATTTA
sdhA_R	AGCTCTGAGTTCAGGAGGTAT
legA3_F	CTCCGCTCTTTCCAGATGAC
legA3_R	GAGTGGGTCGAGTGGGATAA
sidJ_F	GTTGTTCCTACCCAACCTGG
sidJ_R	CAGAGAGGTGTCATGAGTGC

Mariner Tn-seq sequencing library construction

Name	Sequences (5’ to 3’)	Index
First PCR		
Nextera 2A-R	GTCTCGTGGGCTCGGAGATGTGTATAAGAGACAG	
1st_TnR	GTAATACGACTCACTATAGGGTCTAGAG	
Second PCR- Leftward Mariner specific Nextera Indexed primers		
mar147	AATGATACGGCGACCACCGAGATCTACACGCAGGCGGC GTTGACCGGGGACTTATCAGCCAACCTGTTA	GCAGGCGG
mar148	AATGATACGGCGACCACCGAGATCTACACAGGCAGAAC GTTGACCGGGGACTTATCAGCCAACCTGTTA	AGGCAGAA
mar149	AATGATACGGCGACCACCGAGATCTACACCAGAGAGGC GTTGACCGGGGACTTATCAGCCAACCTGTTA	CAGAGAGG
mar150	AATGATACGGCGACCACCGAGATCTACACCGAGGCTGC	CGAGGCTG

	GTTGACCGGGGACTTATCAGCCAACCTGTTA	
mar151	AATGATACGGCGACCACCGAGATCTACACAAGAGGCAC GTTGACCGGGGACTTATCAGCCAACCTGTTA	AAGAGGCA
mar152	AATGATACGGCGACCACCGAGATCTACACGAGGAGCCC GTTGACCGGGGACTTATCAGCCAACCTGTTA	GAGGAGCC
Second PCR- Rightward Mariner specific Nextera Indexed primers		
olk141	CAAGCAGAAGACGGCATACGAGATCCGCCTGCGTCTCGT GGGCTCGGAGATGTG	GCAGGCGG
N703 index	CAAGCAGAAGACGGCATACGAGATTTCTGCCTGTCTCGT GGGCTCGGAGATGTG	AGGCAGAA
Reconditioning		
P1	AATGATACGGCGACCACCGA	
P2	CAAGCAGAAGACGGCATACGA	
Sequencing		
mar512	CGTTGACCGGGGACTTATCAGCCAACCTGTTA	

SI References

1. K. H. Berger, R. R. Isberg, Two distinct defects in intracellular growth complemented by a single genetic locus in Legionella pneumophila. *Mol Microbiol* **7**, 7-19 (1993).
2. K. C. Jeong, J. A. Sexton, J. P. Vogel, Spatiotemporal regulation of a Legionella pneumophila T4SS substrate by the metaeffector SidJ. *PLoS Pathog* **11**, e1004695 (2015).
3. A. W. Ensminger, Y. Yassin, A. Miron, R. R. Isberg, Experimental evolution of Legionella pneumophila in mouse macrophages leads to strains with altered determinants of environmental survival. *PLoS Pathog* **8**, e1002731 (2012).
4. N. A. Ellis, B. Kim, J. Tung, M. P. Machner, A multiplex CRISPR interference tool for virulence gene interrogation in Legionella pneumophila. *Commun Biol* **4**, 157 (2021).
5. J. M. Park, S. Ghosh, T. J. O'Connor, Combinatorial selection in amoebal hosts drives the evolution of the human pathogen Legionella pneumophila. *Nat Microbiol* **5**, 599-609 (2020).
6. J. J. Merriam, R. Mathur, R. Maxfield-Boumil, R. R. Isberg, Analysis of the Legionella pneumophila fliI gene: intracellular growth of a defined mutant defective for flagellum biosynthesis. *Infect Immun* **65**, 2497-2501 (1997).
7. J. Coers, R. E. Vance, M. F. Fontana, W. F. Dietrich, Restriction of Legionella pneumophila growth in macrophages requires the concerted action of cytokine and Naip5/Ipaf signalling pathways. *Cell Microbiol* **9**, 2344-2357 (2007).
8. V. M. Morales, A. Backman, M. Bagdasarian, A series of wide-host-range low-copy-number vectors that allow direct screening for recombinants. *Gene* **97**, 39-47 (1991).
9. T. J. O'Connor, D. Boyd, M. S. Dorer, R. R. Isberg, Aggravating genetic interactions allow a solution to redundancy in a bacterial pathogen. *Science* **338**, 1440-1444 (2012).
10. M. Wan *et al.*, Deubiquitination of phosphoribosyl-ubiquitin conjugates by phosphodiesterase-domain-containing Legionella effectors. *Proc Natl Acad Sci U S A* **116**, 23518-23526 (2019).
11. Y. H. Lin *et al.*, Host Cell-catalyzed S-Palmitoylation Mediates Golgi Targeting of the Legionella Ubiquitin Ligase GobX. *J Biol Chem* **290**, 25766-25781 (2015).
12. R. Kolter, M. Inuzuka, D. R. Helinski, Trans-complementation-dependent replication of a low molecular weight origin fragment from plasmid R6K. *Cell* **15**, 1199-1208 (1978).